2.5.4. Protocol IV: Effects of proteasome activation by IP on the accumulation of ubiquitinated proteins and infarct size in canine hearts

To assess pathophysiological roles of the proteasome in the ischemia/reperfusion myocardium, we intracoronarilly administered saline ($n=9$) or a proteasome inhibitor (epoxomicin at 2.5 μg/kg) ($n=7$) for 50 min and then we performed 90 min of ischemia followed by 6 h of reperfusion in dogs. To assess pathophysiological roles of the proteasome activation by IP in the ischemic/reperfused myocardium, we intracoronarilly administered a proteasome inhibitor (epoxomicin at 2.5 μg/kg) for 50 min with ($n=7$) and without IP ($n=9$) and then we performed 90 min of ischemia followed by 6 h of reperfusion in dogs. We preliminarily confirmed that this dose of epoxomicin reduced 26S proteasome activity by 43.0±6.2% ($n=3$) in the LAD-perfused myocardium compared with that in the LCx-perfused one. After 6 h of reperfusion, we rapidly sampled LAD-perfused myocardium, stored the samples at −80 °C, and investigated the level of the ubiquitinated proteins. We also evaluated the area at risk and the necrotic area after 6 h of reperfusion by Evans blue/TTC staining as described previously [19]. Myocardial infarct size was expressed as the necrotic area/area at risk (Fig. 1).

2.6. Purification of cardiac proteasome

Proteasome was purified from canine hearts according the method reported previously [20]. The peptidase assay was performed using the cytosolic fraction from the LAD- and LCx-perfused myocardium of canine hearts or the fractions containing 26S proteasomes separated on a 10–40% glycerol gradient centrifugation according to the method described above.

2.7. Western blotting analysis

Western blotting analysis was performed as described previously [21]. Immunoreactive bands were quantified by densitometry (Molecular Dynamics).

2.8. Statistical analysis

Data are expressed as the mean±SEM. Proteasome activities in LAD- and LCx-perfused myocardium were compared by the paired *t*-test. The time-course changes in proteasome activity during ischemia/reperfusion myocardium were analyzed by the two-way repeated analysis of variance (ANOVA) followed by Fisher's test. Other results were compared by the one-factor ANOVA followed by Fisher's test. In all analyses, $p<0.05$ was accepted as statistically significant.

3. Results

3.1. PKA enhanced the activity of purified 26S proteasome

The in vitro peptidase assay (Fig. 2A) and the in-gel peptidase assays (Figs. 2B, C) showed that the treatment of purified 26S proteasome with PKA enhanced 26S proteasome activity in a dose-dependent manner, while this effect was blocked by the pretreatment with H-89.

3.2. PKA enhanced the phosphorylation and assembly of purified 26S proteasome

Western blotting analysis of non-reducing gels probed with the antibody against serine/threonine phosphorylated proteins showed that PKA dose-dependently enhanced the phosphorylation of purified 26S proteasome (Figs. 3A, B). The phosphorylation of 26S proteasome was blocked by the pretreatment with H-89 (Figs. 3A, B). Interestingly, Western blotting analysis of non-reducing gels probed with the antibody against Rpt5 or α7 revealed that PKA dose-dependently increased either protein level that corresponded to 26S proteasome, which was blunted by H-89 (Figs. 3C, D upper panel). Western blotting analysis of reducing gels showed that the purified 26S proteasome were equally loaded to each lane (Figs. 3C, D lower panel). These results suggest that PKA enhanced the phosphorylation and assembly of proteasome, which may lead to the increase in proteasome activity.

3.3. PKA stimulation increased 26S proteasome activity in canine hearts

We found no differences in the proteasome activity in the saline-treated (LAD-perfused) and the control (LCx-perfused) myocardium (Fig. 4A). In contrast, exogenous and endogenous PKA stimulation by the selective intracoronary administration of isoproterenol or forskolin and IP, respectively, significantly increased 26S proteasome activity in LAD-perfused myocardium compared with that in LCx-perfused one (Figs. 4B, C, D). The selective intracoronary administration of a PKA inhibitor, H-89, blocked proteasome activation by IP (Fig. 4E). We confirmed that proteasome activation by IP in LCx-perfused myocardium was the same as that in LAD-perfused one (Fig. 4F). These results suggest that exogenous and endogenous PKA stimulation increased 26S proteasome activity in canine hearts.

3.4. PKA stimulation did not alter total protein levels of proteasome subunits in canine hearts

We found no differences in the total protein levels of proteasome subunits in the saline-treated (LAD-perfused) and the control (LCx-perfused) myocardium (Fig. 5A). Then, we examined the changes in protein levels of the proteasome subunits such as Rpt5, α7 and β5 in LAD- and LCx-perfused myocardium when proteasome was activated by exogenous and endogenous PKA stimulation in canine hearts. Importantly, there were no differences in the total protein levels of 3 proteasome subunits (Rpt5, α7, β5) in groups tested (Figs. 5B–F). These results suggest that exogenous and endogenous PKA stimulation did not alter total protein levels of proteasome subunits in the in vivo canine hearts.

3.5. PKA stimulation enhanced 26S proteasome activity and assembly in canine hearts

Since we found 26S proteasome activity of canine hearts mainly in the fractions 17–19 after glycerol gradient centrifugation (Figs. 6A–F, upper panels), samples from fractions 15–21 in the LCx- and LAD-perfused myocardium were immunoblotted with antibodies against Rpt5, α7 or β5 (Figs. 6A–F, lower panels). Consistently, Western blotting analysis with SDS-PAGE gel showed that proteasome subunit Rpt5, α7 or β5 was found mainly in fractions 17–19 (Figs. 6A–F, lower panels).

Fig. 6. Exogenous and endogenous PKA stimulation enhanced 26S proteasome assembly in canine hearts. Representative analysis of 26S proteasome activity (upper panel) and Western blotting analysis of proteasome subunits (lower panel) in the control and treated myocardium. The number indicated fractions separated on a 10–40% glycerol gradient centrifugation. (A) saline, (B) isoproterenol (ISO), (C) forskolin (FOR), (D) ischemic preconditioning (IP), (E) IP with H-89 (IP+H-89), (F) IP in LCx-perfused myocardium. (G) Quantitative analysis of 26S proteasome activity in canine hearts. Proteasome activity was expressed as the summation of proteasome activity in fractions 17–19 in the treatment myocardium which were divided by that in the same fractions in the control one ($n=4$ to 8 each). (H) Quantitative analysis of proteasome assembly in canine hearts. Proteasome assembly was expressed as the summation of Rpt5 protein levels in fractions 17–19 in the treatment myocardium which were divided by that in the same fractions in the control ones ($n=4$ to 8 each). *$p<0.05$ vs sham. #$p<0.05$ vs IP+H-89.

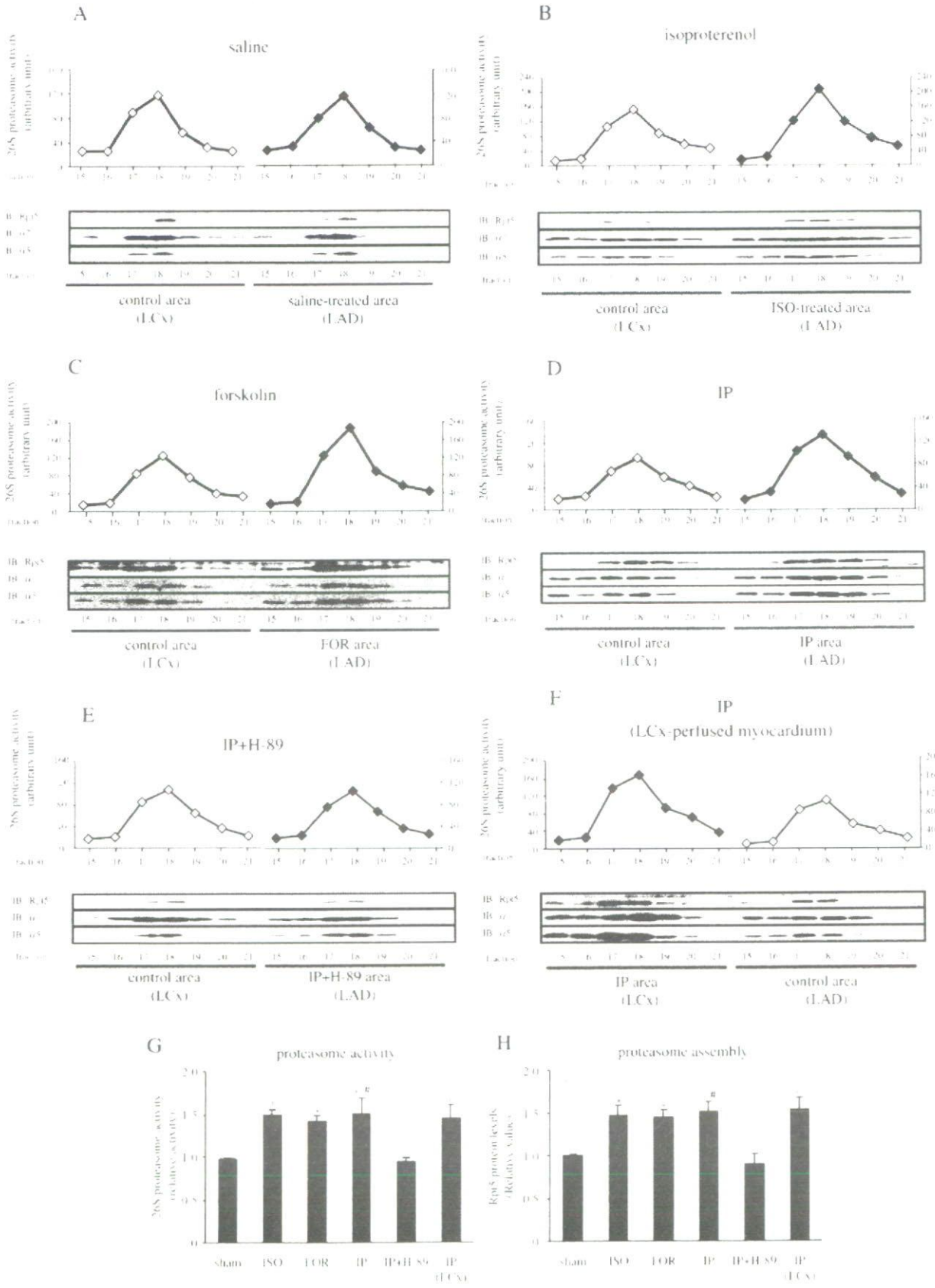
A
saline
control area
(LCx)
saline-treated area
(LAD)
B
isoproterenol
control area
(LCx)
ISO-treated area
(LAD)
C
forskolin
control area
(LCx)
FOR area
(LAD)
D
IP
control area
(LCx)
IP area
(LAD)
E
IP+H-89
control area
(LCx)
IP+H-89 area
(LAD)
F
IP
(LCx-perfused myocardium)
IP area
(LCx)
control area
(LAD)
G
proteasome activity
sham
ISO
FOR
IP
IP+H-89
IP
(LCx)
H
proteasome assembly
sham
ISO
FOR
IP
IP+H-89
IP
(LCx)

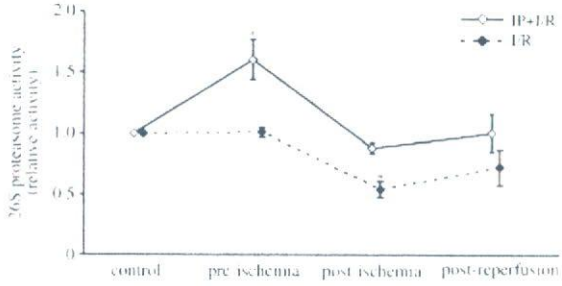

Fig. 7. Time-course changes in proteasome activity during ischemia/reperfusion period. Proteasome activity during ischemia/reperfusion period with and without IP. Myocardial biopsy specimens were taken at the control, just before ischemia (pre-ischemia), at the end of 90 min of ischemia (post-ischemia) and 6 h of reperfusion (post-reperfusion). Proteasome activity in IP+I/R and I/R groups was normalized to the corresponding control ones. IP+I/R and I/R indicate ischemia/reperfusion with and without IP, respectively. $^{*}p<0.05$ vs control at the corresponding group.

Fig. 6 showed the representative proteasome activity and assembly using the myocardial sample of canine-1 in each groups in Fig. 5. Since we confirmed that the total amount of proteasome subunits were same in the control and treated myocardium, the alteration in protein levels of proteasome subunits in proteasome enriched fractions 17–19 indicate the alternation in the status of proteasome assembly. No differences were found in protein levels of proteasome subunits in the saline-treated (LAD-perfused) and the control (LCx-perfused) myocardium (Fig. 6A). Importantly, along with the increase in proteasome activity, the exogenous and endogenous PKA stimulation by isoproterenol, forskolin and IP significantly increased the protein levels of 3 different proteasome subunits in fractions 17–19 in the LAD-perfused myocardium compared with those in LCx-perfused one (Figs. 6B–D). Moreover, the selective administration of H-89 blunted the increases in protein levels of 3 different proteasome subunits and proteasome activation by IP in fractions 17–19 in the LAD-perfused myocardium (Fig. 6E). We also confirmed that the same findings were induced by IP in LCx-perfused myocardium (Fig. 6F). Quantitative analysis also showed that PKA enhanced proteasome activity and assembly, both of which were expressed as the summation of proteasome activity and Rpt5 protein levels in fractions 17–19 in the treatment myocardium which were divided by that in the same fractions in the control one, respectively (Figs. 6G, H). These results suggest that PKA stimulation enhanced 26S proteasome assembly and activity in canine hearts without alteration of total protein levels of proteasome subunits.

3.6. Time-course changes in proteasome activity during ischemia/reperfusion period with and without IP

The analysis of consecutive myocardial biopsy samples also revealed that IP increased the proteasome activity in the LAD-perfused myocardium in the same dog (Fig. 7). In canine hearts with IP, the proteasome activities at the post-ischemia and post-reperfusion were significantly lower than that at the pre-ischemia (=just after IP), but they did not differ from the control. In canine hearts without IP, the proteasome activity at the post-ischemia was significantly decreased compared with that at the control or pre-ischemia (Fig. 7). Myocardial proteasome activity at the post-reperfusion did not differ from that at the post-ischemia in groups with and without IP (Fig. 7).

3.7. IP blunted the accumulation of ubiquitinated proteins in ischemia/reperfusion myocardium

To examine the pathophysiological role of proteasome activation by IP, we investigated effects of IP on the accumulation of ubiquitinated proteins, which may predict recovery of postischemic cardiac function [22], in the ischemia/reperfusion myocardium in canine model. Western blotting analysis revealed that ubiquitinated proteins were increased in ischemia/reperfusion myocardium, while their accumulation was attenuated by IP (Figs. 8A, B). The reduction in

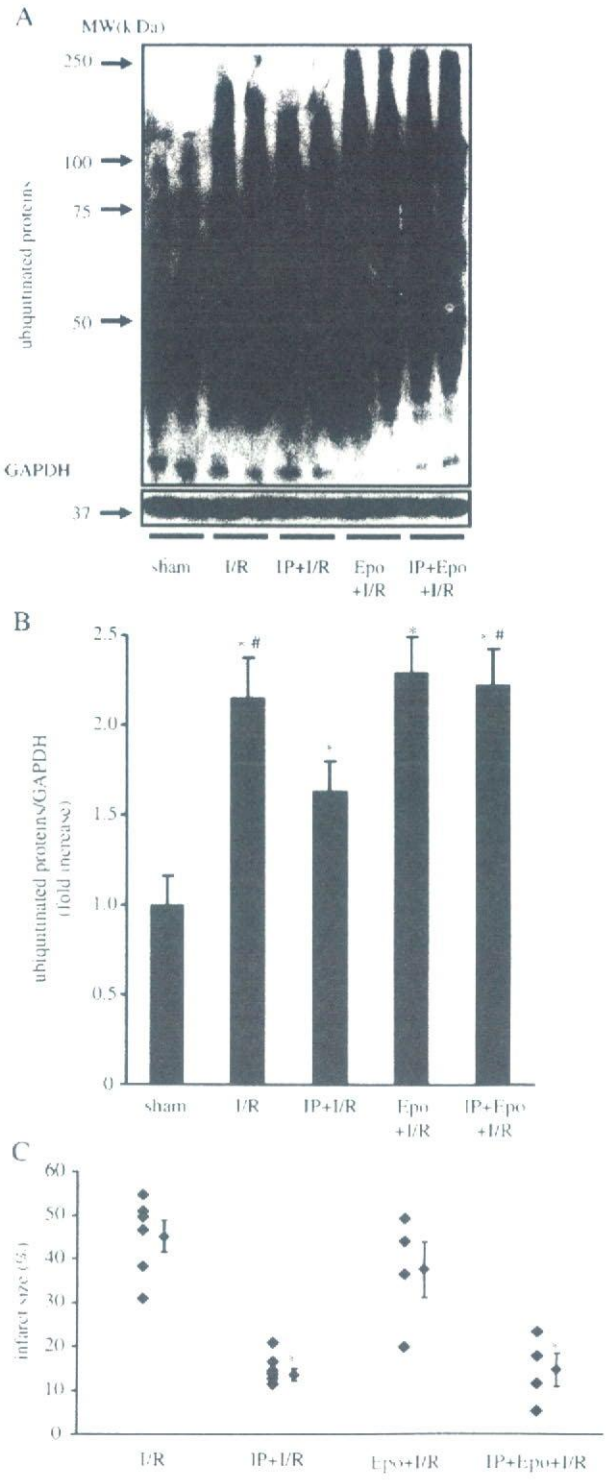

Fig. 8. Pathophysiological role of the enhancement of proteasome activity by IP. Representative example (A) and quantitative analysis (B) of Western blotting analysis of ubiquitinated proteins in canine ischemia/reperfusion (I/R) myocardium. $^{*}p<0.05$ vs. sham, #$p<0.05$ vs. IP+I/R. $n=3$ per group. Values were normalized to sham. (C) Myocardial infarct size. $^{*}p<0.05$ vs. I/R. MW, IP and Epo indicate molecular weight, ischemic preconditioning and epoxomicin (a proteasome inhibitor), respectively.

accumulated ubiquitinated proteins by IP was blunted by a proteasome inhibitor, epoxomicin. These results indicate that proteasome activation by IP alleviated the accumulation of ubiquitinated proteins in canine ischemia/reperfusion hearts.

3.8. Proteasome inhibition did not alter infarct size in canine hearts with and without IP

Fig. 8C showed the infarct size for each group in protocol IV. The intracoronary administration of epoxomicin before ischemia did not alter infarct size in this canine model. Consistent with the previous reports [15], we found that IP reduced myocardial infarct size. The infarct size-limiting effects of IP were not affected by the intracoronary administration of epoxomicin during IP procedure.

4. Discussion

4.1. PKA rapidly enhances phosphorylation, assembly and activity of 26S purified proteasome

Proteasome regulates cellular functions by eliminating ubiquitinated proteins [1–4]. Proteasome activity is enhanced by an increase in the levels of proteasome subunit proteins and their assembly, as well as by the post-translational modification of proteasome subunit through processes such as phosphorylation/dephosphorylation [9,10]. Recent studies have shown that PKA can phosphorylate several sites and increase proteasome activity in vitro [11,12]. Furthermore, although the involvement of PKA is not shown, the phosphorylation of proteasome subunits alters the status of proteasome assembly [23,24]. In the present study, we firstly showed that PKA activation enhanced the proteasome assembly, which contributed to the increase in proteasome activity. These findings suggest that altering proteasome subunit configuration through directed assembly by PKA may lead to the increase in proteasome activity, although we cannot exclude the possibility that PKA-mediated phosphorylation of proteasome subunits directly activates proteasome. Further investigation will be needed to clarify what subunit of proteasome is phosphorylated by PKA and the direct association between phosphorylation and assembly.

4.2. PKA stimulation enhances assembly and activity in in vivo canine hearts without affecting the total protein levels of proteasome subunits

Since proteasome activity is regulated by the multiple factors such as intracellular ATP levels and post-translational modification of proteasome [9,10], the in vitro findings of proteasome regulation are not always applied in the vivo model. Thus, to clarify whether the in vitro findings were also valid in vivo, we examined whether PKA stimulation could modulate proteasome assembly and activity in canine hearts. We employed two maneuvers to activate PKA in vivo, which were isoproterenol and forskolin as an exogenous stimulant of PKA [18,25] and IP as an endogenous stimulant [15]. We confirmed that both exogenous and endogenous stimulation of PKA enhanced 26S proteasome activity at 30 min after administration without changing the total protein levels of proteasome subunits in in vivo canine hearts. To our knowledge, the present study is the first to show the intervention to increase proteasome activity in vivo, suggesting that the pathophysiological conditions due to proteasome dysfunction in hearts could be treated.

We have found both 20S (α7 and β5) and 19S (Rpt5) subunit proteins in fractions where proteasome activity was detected, indicating that 26S proteasome was indeed eluted in these fractions. We confirmed that exogenous and endogenous PKA stimulation increased the protein levels of proteasome subunits in these fractions without changing total amount of proteasome subunits. These findings suggest that PKA stimulation enhanced 26S proteasome assembly as well as activity in in vivo canine hearts.

4.3. Time-course changes in proteasome activity during ischemia/reperfusion period with and without IP

To examine the time-course changes in proteasome activity during ischemia/reperfusion period, we performed myocardial biopsy at 4 time-points during ischemia/reperfusion period: at the control, just before ischemia (pre-ischemia), at the end of 90 min ischemia (post-ischemia) and 6 h of reperfusion (post-reperfusion). Previous study indicated that proteasome activity was decreased after ischemia/reperfusion [8]. Consistent with the previous report, the proteasome activity at the post-ischemia was significantly decreased compared with that at the control or pre-ischemia in groups without IP. Meanwhile, the proteasome activity at the post-ischemia was significantly lower than that at the pre-ischemia (=just after IP), however, it did not differ from the control in groups with IP (Fig. 7). These findings suggest that stimuli during ischemic period decreased myocardial proteasome activity and that proteasome activation by IP during ischemic period may play an important role in the protein turnover and cellular functions in ischemia/reperfusion hearts. Myocardial proteasome activity at the end of reperfusion did not differ from that at the end of ischemia in groups with and without IP, suggesting that stimuli during reperfusion did not significantly affect proteasome activity. Unfortunately, due to the small volume of biopsy samples, we could not check the time-course changes in the status of proteasome assembly.

4.4. IP blunts the accumulation of ubiquitinated proteins in ischemia/reperfusion myocardium

Recently, the ubiquitination of proteins is important post-translational processes that modify the functions of many proteins. We and others have reported that the accumulation of ubiquitinated protein in hearts was associated with the progression of cardiac dysfunction due to apoptosis [7,26]. In addition, the injured myocardium by ischemia/reperfusion is concomitant with a reduced proteasome activity [8]. Consistent with these previous reports, we found the decreased proteasome activity and the accumulation of ubiquitinated proteins in the ischemia/reperfusion myocardium. Interestingly, we found the less accumulation of ubiquitinated proteins in ischemia/reperfusion myocardium, which may be attributable to the 40% increase in proteasome activity by endogenous PKA stimulation. Since the accumulation of ubiquitinated proteins may predict recovery of postischemic cardiac function [21], the removal of damaged proteins due to proteasome activation by IP may contribute to improve postischemic cardiac function.

4.5. Proteasome inhibition did not alter infarct size in canine hearts with and without IP

Finally, we examined whether proteasome activation by IP contributed to its infarct-size limiting effects in the canine model. The infarct-size limiting effects of IP were not prevented by the intracoronary administration of epoxomicin, a proteasome inhibitor, at the dose that reduces proteasome activity by 43%. These findings suggest that proteasome activation by IP was not involved in the infarct-size limiting effects of IP in the acute phase. Future studies will be required about the pathophysiological role of proteasome activation in the chronic phase after myocardial infarction. Moreover, the intracoronary administration of epoxomicin itself could not reduce the infarct size in this model. This data was inconsistent with the previous ones that the inhibition of proteasome could reduce myocardial infarct size in rats and pigs [27,28]. The discrepancy between the previous and our studies might be due to the differences in animals used, experimental protocols and the drugs used. Further investigation will be needed to clarify whether reduced proteasome activity is beneficial or detrimental in the ischemia/reperfusion injury in the acute phase.

In conclusion, the present study demonstrated that PKA rapidly enhances proteasome activity and assembly in the in vivo heart. Modulation of proteasome activity and assembly might be a promising new therapeutic approach for cardiovascular diseases.

Acknowledgments

We thank Saori Ikezawa and Yoko Hamada for their technical assistance, and Kieko Segawa for the secretarial work. This work is supported by Grants-in-aid from the Ministry of Health, Labor, and Welfare-Japan and Grants-in-aid from the Ministry of Education, Culture, Sports, Science and Technology-Japan and Grants from the Japan Heart Foundation and Grants from the Japan Cardiovascular Research Foundation.

References

[1] Hershko A, Ciechanover A. The ubiquitin system. Annu Rev Biochem 1998;67:425–79.
[2] Hochstrasser M. Ubiquitin, proteasomes, and the regulation of intracellular protein degradation. Curr Opin Cell Biol 1995;7:215–23.
[3] Glickman MH, Ciechanover A. The ubiquitin–proteasome proteolytic pathway: destruction for the sake of construction. Physiol Rev 2002;82:373–428.
[4] Powell SR. The ubiquitin–proteasome system in cardiac physiology and pathology. Am J Physiol Heart Circ Physiol 2006;291:H1–H19.
[5] Voges D, Zwickl P, Baumeister W. The 26S proteasome: a molecular machine designed for controlled proteolysis. Annu Rev Biochem 1999;68:1015–68.
[6] DeMartino GN, Slaughter CA. The proteasome, a novel protease regulated by multiple mechanisms. J Biol Chem 1999;274:22123–6.
[7] Tsukamoto O, Minamino T, Okada K, Shintani Y, Takashima S, Kato H, et al. Depression of proteasome activities during the progression of cardiac dysfunction in pressure-overloaded heart of mice. Biochem Biophys Res Commun 2006;340:1125–33.
[8] Bulteau AL, Lundberg KC, Humphries KM, Sadek HA, Szweda PA, Friguet B, et al. Oxidative modification and inactivation of the proteasome during coronary occlusion/reperfusion. J Biol Chem 2001;276:30057–63.
[9] Zolk O, Schenke C, Sarikas A. The ubiquitin–proteasome system: focus on the heart. Cardiovasc Res 2006;70:410–21.
[10] Wang X, Robbins J. Heart failure and protein quality control. Circ Res 2006;99:1315–28.
[11] Zong C, Gomes AV, Drews O, Li X, Young GW, Berhane B, et al. Regulation of murine cardiac 20S proteasomes: role of associating partners. Circ Res 2006;99:372–80.
[12] Zhang F, Hu Y, Huang P, Toleman CA, Paterson AJ, Kudlow JE. Proteasome function is regulated by cyclic AMP-dependent protein kinase through phosphorylation of Rpt6. J Biol Chem 2007;282:22460–71.
[13] Wang Z, Aris VM, Ogburn KD, Soteropoulos P, Figueiredo-Pereira ME. Prostaglandin J2 alters pro-survival and pro-death gene expression patterns and 26 S proteasome assembly in human neuroblastoma cells. J Biol Chem 2006;281:21377–86.
[14] Fujita M, Asanuma H, Hirata A, Wakeno M, Takahama H, Sasaki H, et al. Prolonged transient acidosis during early reperfusion contributes to the cardioprotective effects of postconditioning. Am J Physiol Heart Circ Physiol 2007;292:H2004–8.
[15] Sanada S, Asanuma H, Tsukamoto O, Minamino T, Node K, Takashima S, et al. Protein kinase A as another mediator of ischemic preconditioning independent of protein kinase C. Circulation 2004;110:51–7.
[16] Sanada S, Kitakaze M, Papst PJ, Asanuma H, Node K, Takashima S, et al. Cardioprotective effect afforded by transient exposure to phosphodiesterase III inhibitors: the role of protein kinase A and p38 mitogen-activated protein kinase. Circulation 2001;104:705–10.
[17] Minamino T, Kitakaze M, Asanuma H, Tomiyama Y, Shiraga M, Sato H, et al. Endogenous adenosine inhibits P-selectin-dependent formation of coronary thromboemboli during hypoperfusion in dogs. J Clin Invest 1998;101:1643–1653.
[18] Kitakaze M, Hori M, Sato H, Takashima S, Inoue M, Kitabatake A, et al. Endogenous adenosine inhibits platelet aggregation during myocardial ischemia in dogs. Circ Res 1991;69:1402–8.
[19] Ogita H, Node K, Asanuma H, Sanada S, Liao Y, Takashima S, et al. Amelioration of ischemia- and reperfusion-induced myocardial injury by the selective estrogen receptor modulator, raloxifene, in the canine heart. J Am Coll Cardiol 2002;40:998–1005.
[20] Gomes AV, Zong C, Edmondson RD, Li X, Stefani E, Zhang J, et al. Mapping the murine cardiac 26S proteasome complexes. Circ Res 2006;99:362–71.
[21] Minamino T, Gaussin V, DeMayo FJ, Schneider MD. Inducible gene targeting in postnatal myocardium by cardiac-specific expression of a hormone-activated Cre fusion protein. Circ Res 2001;88:587–92.
[22] Powell SR, Wang P, Katzeff H, Shringarpure R, Teoh C, Khaliulin I, et al. Oxidized and ubiquitinated proteins may predict recovery of postischemic cardiac function: essential role of the proteasome. Antioxid Redox Signal 2005;7:538–546.
[23] Satoh K, Sasajima H, Nyoumura KI, Yokosawa H, Sawada H. Assembly of the 26S proteasome is regulated by phosphorylation of the p45/Rpt6 ATPase subunit. Biochemistry 2001;40:314–9.
[24] Bose S, Stratford FL, Broadfoot KI, Mason GG, Rivett AJ. Phosphorylation of 20S proteasome alpha subunit C8 (alpha7) stabilizes the 26S proteasome and plays a role in the regulation of proteasome complexes by gamma-interferon. Biochem J 2004;378:177–84.
[25] Mutafova-Yambolieva VN, Smyth L, Bobalova J. Involvement of cyclic AMP-mediated pathway in neural release of noradrenaline in canine isolated mesenteric artery and vein. Cardiovasc Res 2003;57:217–24.
[26] Powell SR, Gurzenda EM, Teichberg S, Mantell LL, Maulik D. Association of increased ubiquitinated proteins with cardiac apoptosis. Antioxid Redox Signal 2000;2:103–12.
[27] Pye J, Ardeshirpour F, McCain A, Bellinger DA, Merricks E, Adams J, et al. Proteasome inhibition ablates activation of NF-kappa B in myocardial reperfusion and reduces reperfusion injury. Am J Physiol Heart Circ Physiol 2003;284:H919–26.
[28] Campbell B, Adams J, Shin YK, Lefer AM. Cardioprotective effects of a novel proteasome inhibitor following ischemia and reperfusion in the isolated perfused rat heart. J Mol Cell Cardiol 1999;31:467–76.

Available online at www.sciencedirect.com
ScienceDirect
Biochemical and Biophysical Research Communications 365 (2008) 541–547
BBRC
www.elsevier.com/locate/ybbrc

Identification of a novel substrate for TNFα-induced kinase NUAK2

Hiroyuki Yamamoto [a], Seiji Takashima [b,c,*], Yasunori Shintani [b], Satoru Yamazaki [d], Osamu Seguchi [d], Atsushi Nakano [d], Shuichiro Higo [b], Hisakazu Kato [b], Yulin Liao [d], Yoshihiro Asano [b], Tetsuo Minamino [b], Yasushi Matsumura [a], Hiroshi Takeda [a], Masafumi Kitakaze [d]

[a] *Department of Medical Information Science, Osaka University Graduate School of Medicine, Suita, Osaka 565-0871, Japan*
[b] *Department of Cardiovascular Medicine, Osaka University Graduate School of Medicine, 2-2 Yamadaoka, Suita, Osaka 565-0871, Japan*
[c] *Health Care Center, Osaka University Graduate School of Medicine, Suita, Osaka 565-0871, Japan*
[d] *Department of Cardiovascular Medicine, National Cardiovascular Center, Suita, Osaka 565-8565, Japan*

Received 2 November 2007
Available online 20 November 2007

Abstract

TNFα has multiple important cellular functions both in normal cells and in tumor cells. To explore the role of TNFα, we identified NUAK family, SNF1-like kinase 2 (NUAK2), as a TNFα-induced kinase by gene chip analysis. NUAK2 is known to be induced by various cellular stresses and involved in cell mortality, however, its substrate has never been identified. We developed original protocol of de novo screening for kinase substrates using an in vitro kinase assay and high performance liquid chromatography (HPLC). Using this procedure, we identified myosin phosphatase target subunit 1 (MYPT1) as a specific substrate for NUAK2. MYPT1 was phosphorylated at another site(s) by NUAK2, other than known Rho-kinase phosphorylation sites (Thr696 or Thr853) responsible for inhibition of myosin phosphatase activity. These data suggests different phosphorylation and regulation of MYPT1 activity by NUAK2.

Keywords: NUAK family, SNF1-like kinase 2 (NUAK2); Myosin phosphatase target subunit 1 (MYPT1); TNFα; Myosin phosphatase; In vitro kinase assay

Tumor necrosis factor (TNFα) has multiple cellular functions both in normal cells and in tumor cells. TNFα not only induces apoptotic cell death but also enhances various gene expressions mediated by NFκB family transcriptional factors. Endothelial cells express TNFα receptors, and its NFκB-mediated signals induce various chemokine related molecules and cell adhesion molecules. These molecules enhance attachment of mononuclear cells and help these cells to enter into inflammatory tissues through endothelial cell barrier. TNFα also induces chemotactic molecules of endothelial cell, indicating that cell mobility induced by TNFα signal is mediated by as yet unidentified molecular mechanisms [1].

In the current study, we demonstrated that NUAK family, SNF1-like kinase 2 (NUAK2) was identified as a TNFα-induced kinase in endothelial cells by gene chip analysis. NUAK2 was originally identified in a PCR-based screen designed to identify a novel protein kinase [2]. Subsequent studies indicated that NUAK2 was induced by various cellular stresses such as ER stress, elevation of cellular AMP, hyperosmotic stress, and ultraviolet [3]. High expression of NUAK2 was also confirmed in various tumor cell lines [4], and overexpression of NUAK2 was reported to render tumor cell resistance under apoptotic stimuli. Such inductions and expressional mechanisms of NUAK2 have

* Corresponding author. Address: Department of Cardiovascular Medicine, Osaka University Graduate School of Medicine, 2-2 Yamadaoka, Suita, Osaka 565-0871, Japan. Fax: +81 6 8679 3473.
E-mail address: takasima@medone.med.osaka-u.ac.jp (S. Takashima).

0006-291X/$ - see front matter © 2007 Elsevier Inc. All rights reserved.
doi:10.1016/j.bbrc.2007.11.013

been well reported, however its substrate has never been identified.

Diverse effects of kinases in various tissues depend on specific substrates. To reveal the function of kinase it is essential to purify its substrate. Here, we identified myosin phosphatase target subunit 1 (MYPT1) as a specific substrate for NUAK2 using unique purification procedure. This method was designed to purify target substrates by combination of an in vitro kinase assay and high performance liquid chromatography (HPLC). NUAK2 phosphorylated MYPT1 at a distinct site(s) other than known Rho-kinase (ROCK) phosphorylation sites (Thr696 or Thr853) responsible for inhibition of myosin phosphatase activity, suggesting different phosphorylation and regulation of MYPT1 activity by NUAK2.

Materials and methods

Cell lines and reagents. Human umbilical vein endothelial cells (HUVECs) and human aortic smooth muscle cells (AoSMCs) were obtained from Clonetics. They were cultured in endothelial and smooth muscle cell medium (Clonetics) and used up to passage 5. HEK293T cells and HeLa cells were cultured in DMEM with 10% FBS. The following antibodies were purchased: anti-Flag (M2Ab; Sigma), anti-V5 (Invitrogen), anti-Myc (Invitrogen), anti-Tubulin (Cell Signaling), anti-NUAK2 (Abgent), anti-MYPT1 (BD Biosciences), anti-phospho-MYPT1 (Thr696) (Upstate Biotechnology), and anti-phospho-MYPT1 (Thr853) (CycLex). The following reagents were purchased: Trypsin (Promega), Lipofectamine 2000 (Invitrogen), Flag peptide (Sigma), and human recombinant TNFα (R&D Systems, Inc.).

cDNA microarray analysis. To determine the effect of TNFα on gene expression profile, we treated cultured HUVECs without or with TNFα (20 ng/ml) for 2 h, and then performed cDNA microarray studies. Total RNA was prepared from HUVECs using RNA-Bee-RNA Isolation Reagent (Tel-Test Inc.) according to the manufacturer's instructions. Microarray hybridization was performed in triplicate using Affymetrix Human Genome 133A gene chips (HG-U133A). After synthesizing double-stranded cDNA from the total RNA, an in vitro transcription reaction was done to produce biotin-labeled cRNA from cDNA, and the cRNA was fragmented before hybridization. Hybridization, probe washing, staining and probe array scanning were performed following the protocols provided by Affymetrix. Data were analyzed using Genespring 6 software [5]. Normalization was done by a combination of three steps: rewriting negative values as 0.01, normalizing to the 50th percentile per chip and normalizing to the median per gene. We filtered data using a combination of parameters such as signal confidence ('present' flag), fold change (>3), minimum acceptable signal intensity (average difference ⩾50 in at least one of the two groups). Indicated gene accession numbers were derived from the GenBank database.

Northern blot analysis. Northern blot analysis was performed as previously described [6]. Briefly, total RNA was isolated and electrophoresed on 1% agarose gel containing 2.2 M formaldehyde, and transferred onto nylon membranes (Bio-Rad). The membranes were hybridized with ^{32}P-labeled fragments of human cDNA corresponding to nucleotides 1–1887 of NUAK2 cDNA. A BAS photoimaging system (Fuji) was used for detection.

Quantitative RT–PCR. Total RNA was extracted using RNA-Bee-RNA Isolation Reagent (Tel-Test Inc.). Then, 1 μg of total RNA was reverse-transcribed using Omniscript RT (Qiagen) according to the manufacturer's protocol. Quantitative RT-PCR was performed with TaqMan technology using the ABI Prism 7000 detection system (Applied Biosystems) according to the manufacturer's instructions. RT-PCR conditions were 2 min at 50 °C, 10 min at 95 °C, and 40 cycles of 15 s at 95 °C and 1 min at 60°C. Data were normalized to 18S ribosomal RNA or GAPDH level. Each sample was analyzed in duplicate and the experiments were replicated three times. For 18S ribosomal RNA, GAPDH and NUAK2, primers and probes were obtained using TaqMan Assays-on-Demand gene expression products (Applied Biosystems).

Cloning, plasmid construction, and mutagenesis. In this experiment, all construction was performed using the Gateway system (Invitrogen) according to the manufacturer's instructions. Human NUAK2 cDNA was isolated from HUVECs cDNA using the following sense and antisense primers: sense 5′ caccatggagtcgctggtttttcg and antisense 5′ tcaggtgagctttgagcagaccc. With PCR primer designed to include stop codon of NUAK2, the amplified fragment was inserted into pENTR/D-TOPO (Invitrogen), named pENTR/NUAK2. To generate N-terminal Flag-tagged NUAK2 (Flag-NUAK2), Flag epitope (DYKDDDDK) was introduced into just before the N terminus of NUAK2 by PCR-based mutagenesis using pENTR/NUAK2 as a template. The NUAK2 constructs were recombined to mammalian expression vector, pcDNA3.1 vector (Invitrogen). We also generated N-terminal Myc-tagged NUAK2 (Myc-NUAK2) using the same protocol. cDNA encoding human MYPT1 was generated by RT-PCR with RNA from HUVECs. The mammalian expression vectors for MYPT1 were constructed using pENTR/D-TOPO (pENTR-MYPT1). To identify the binding site on MYPT1 for NUAK2, pENTR-Flag-MYPT1 D1 lacking aa 11–286, pENTR-Flag-MYPT1 D2 lacking aa 287–514, pENTR-Flag-MYPT1 D3 lacking aa 515–799 or pENTR-Flag-MYPT1 D4 lacking aa 800–1020 were generated by PCR using pENTR-MYPT1 as a template. An *Escherichia coli* expression vector for GST-MYPT1 was constructed using the expression vector, pGEX5X-1 (Pharmacia) and cDNA encoding MYPT1 protein. Expression plasmids for mutated NUAK2 and mutated MYPT1 were generated using the QuickChange site-directed mutagenesis kit (Stratagene) following the manufacturer's instructions. All constructs were verified by sequencing.

Co-immunoprecipitation assay. HEK293T cells were transfected with 5 μg cDNA/60 mm dish using Lipofectamine 2000. Two days after transfection, cells were lysed in lysis buffer (1% Nonidet P-40, 0.15 M NaCl, 20 mM Tris, pH 7.2, and 2 mM EDTA including protease inhibitor cocktail (Nacalai)). We then incubated with anti-V5, anti-Myc or anti-Flag agarose for 1 h at 4 °C. After extensive washing, immunoprecipitated samples were subjected to SDS–PAGE and immunoblotting was performed as described previously [7].

In vitro kinase assay. The following recombinant proteins were purchased: human NUAK2 (Cell Signaling), and ROCK-II, human active (Upstate Biotechnology). Bacterially purified glutathione S-transferase (GST) fusing proteins were used as substrates. Recombinant proteins were equilibrated in kinase buffer [0.15 M NaCl, 20 mM MOPS (pH 7.0), 10 μM $MgCl_2$, 10% glycerol, and 1 mM DTT], and then incubated with 10 μCi of [γ-^{32} P] ATP (Amersham) and substrates at 30 °C for 60 min. Each sample was boiled in SDS sample buffer for 3 min, and eluted proteins were analyzed by SDS–PAGE. The gel was dried and autoradiographed. ROCK-II, human active (0.317 pmol) and NUAK2 (1.33 pmol) were used in this assay.

Identification of a NUAK2-binding protein (p130). We used HEK293T cells expressing pcDNA3.1-Flag-tagged-NUAK2, lysed them with 1 ml of lysis buffer and immunoprecipitated them with anti-Flag antibody followed by elution with Flag peptide (100 μg/ml). An in vitro kinase assay was performed with the eluate in the presence of [γ-^{32}P] ATP followed by SDS–PAGE, and the radioactivity was detected by a BAS imaging analyzer (Fuji). The FLAG peptide eluate was injected onto a phenyl-reverse phase—HPLC column (4.6 × 250 mm, Nacalai) equilibrated with 0.1% trifluoroacetic acid and 5% acetonitrile. Fractions were eluted with a linear gradient of 35–45% acetonitrile at a flow rate of 1 ml/min. Each fraction was lyophilized and separated by SDS–PAGE. Radioactivity was detected by BAS imaging system.

Data analysis. Statistical significance was assessed with ANOVA using the Fisher's post hoc test. A value of $p < 0.05$ was considered to be statistically significant.

Table 1
Expression levels and fold change of the upregulated genes by TNFα in HUVECs (top 20)

Gene name	Accession No.	Control group	TNFα group	Fold change (TNFα/Control)
CCL20	NM_004591.1	0.04	7.33	168.20
E-selectin	NM_000450.1	0.08	5.11	70.63
IL-8	NM_000584.1	0.16	8.16	50.35
Coagulation factor III	NM_001993.2	0.29	7.17	24.96
TNFAIP3	NM_006290.1	0.21	4.08	19.05
VCAM1	NM_001078.1	0.16	3.03	18.95
CXCL3	NM_002090.1	0.27	5.07	18.46
CXCL2	NM_002089	0.34	4.99	14.68
TNFAIP2	NM_006291.1	0.26	3.55	13.52
CXCL1	NM_001511.1	0.32	3.70	11.70
CXCR7	NM_020311	0.37	4.02	10.77
ICAM1	NM_000201.1	0.23	2.36	10.34
TNFAIP8	NM_014350.1	0.50	5.01	9.95
Ephrin-A1	NM_004428.1	0.26	2.24	8.63
CD69 antigen	NM_001781.1	0.53	3.93	7.43
CX3CL1	NM_002996	0.36	2.46	6.75
RND1	NM_014470	0.32	2.04	6.37
PMAIP1	NM_021127.1	0.73	4.58	6.26
NUAK2	NM_030952.1	0.31	1.91	6.24
CCL2	NM_002982	0.42	2.47	5.87

HUVECs were stimulated with TNFα (20 ng/ml) (TNFα group) or medium only (Control) for 2 h. Every time, a pair of TNFα and Control was used for cDNA microarray examination, which was repeated for three times in different date. Data are mean for the three times. Only the genes that were upregulated by TNFα for more than 3-folds every times were included in this table. The expression levels were normalized intensity (linear scale).

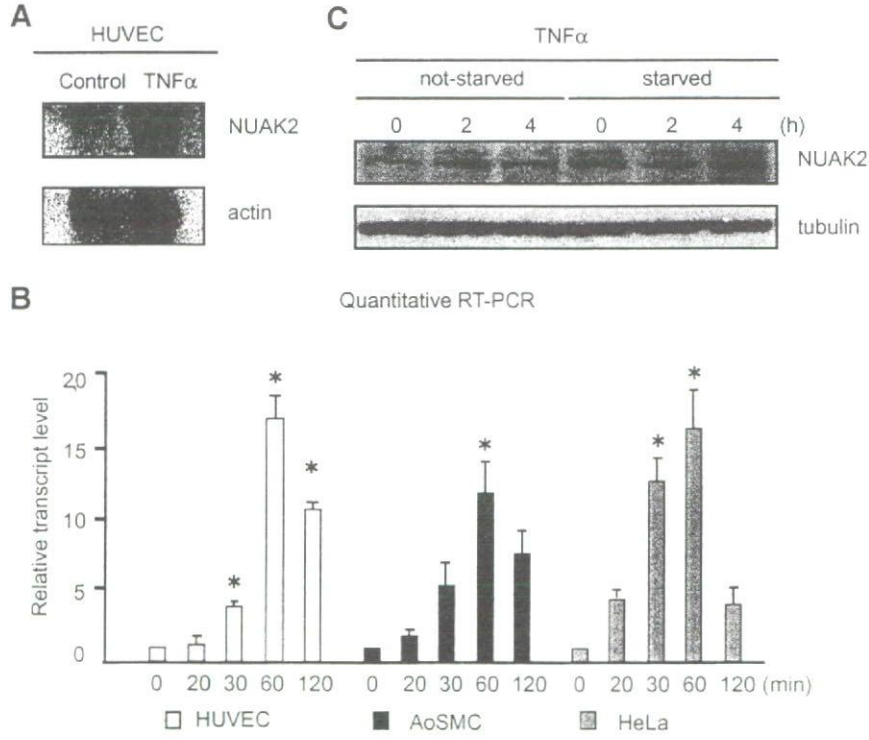

Fig. 1. TNFα induces upregulation of human NUAK2 expression. (A) Northern blot analysis. HUVECs were treated with TNFα (20 ng/ml) for 2 h or control. Total RNA was harvested, electrophoresed, and blotted to the nitrocellulose membrane. The membrane was probed with cDNA for human NUAK2. Beta actin was used as an internal control for mRNA loading. (B) Time course of NUAK2 mRNA levels. Various cell lines were treated with TNFα (20 ng/ml) for the indicated times. Each sample was analyzed in duplicate and experiments were performed in triplicate. (C) HeLa cells were either not starved or starved for 18 h in DMEM containing 0.5% serum. Starved and unstarved cells were then treated with TNFα (20 ng/ml) for indicated times. Cells were lysed and immunoblotting was performed with the indicated antibodies. For panels B, error bars represent SEM. $^{*}P < 0.05$ versus baseline.

Results

TNFα induced NUAK2 mRNA and protein expressions

To identify the specific expression targets of TNFα, the profiles of mRNA expression extracted from HUVECs were analyzed. Triplicate assay of gene chip revealed that 57 genes were enhanced their expressions 2 h after TNFα treatment. Most of these genes increased more than 3-folds are chemokines and their related molecules such as their receptors, adhesion molecules, and transcription factors (Table 1). Among them, one kinase, NUAK2, was greatly enhanced its expression by TNFα. No other kinases were enhanced its expression more than 3-folds, suggesting that NUAK2 is only a strongly inducible kinase by TNFα signaling in endothelial cells. This result was confirmed by Northern blot analysis (Fig. 1A). Quantitative PCR revealed that an enhanced NUAK2 expression after TNFα treatment was seen not only in HUVECs but also in other cell lines in a time-dependent manner (Fig. 1B). Increasing protein level by TNFα was also confirmed by immunoblotting with anti-NUAK2 antibody (Fig. 1C).

NUAK2-associated kinase activity

Since the substrate for NUAK2 has not been identified, we screened a protein which bound to NUAK2 and was phosphorylated by NUAK2. We employed a kinase-dead construct of NUAK2 (Flag-KD-NUAK2) in which Lys81 was replaced with Arg as a control. HEK293T cells were transiently transfected with Flag-WT-NUAK2 or Flag-KD-NUAK2. Immunoprecipitation assay was performed with whole-cell extracts using anti-Flag antibody followed by elution with Flag peptide. An in vitro kinase assay was performed with the eluate in the presence of [γ-^{32}P] ATP. NUAK2 was autophosphorylated in vitro [4]. Besides NUAK2 radioactivity, a phosphorylated band at the size of 130 kDa (p130) was co-immunoprecipitated

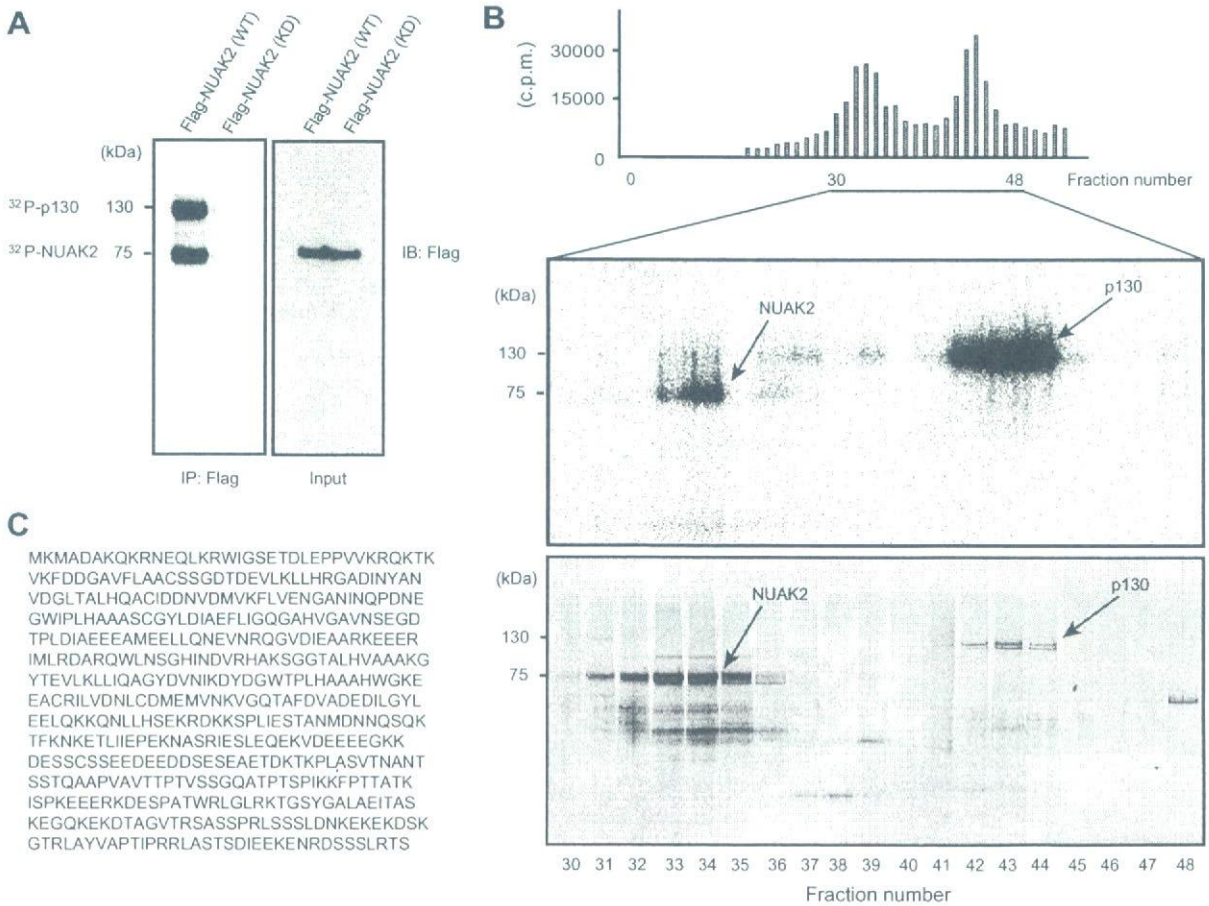

Fig. 2. Purification and identification of MYPT1. (A) HEK293T cells were transiently transfected with Flag-WT-NUAK2 or Flag-KD-NUAK2. Immunoprecipitation assay was performed with whole-cell extracts using anti-Flag antibody followed by elution with Flag peptide. An in vitro kinase assay was performed with the eluate in the presence of [γ-^{32}P] ATP (left panel). The lysates were immunoblotted with anti-Flag antibody (right panel). (B) The complex of radiolabeled NUAK2 and p130 was separated by a phenyl reverse-phase column and indicated fractions were quantified for phosphorylation of the complex (upper panel). These proteins in the indicated fractions were resolved by SDS–PAGE followed by autoradiography (middle panel). Large-scale purification of the protein complex was done using the same protocol without radioactive material. The purified products of the protein complex were resolved on SDS–PAGE and silver stained (lower panel). (C) Amino acid sequence of human MYPT1. The peptides derived from the purified protein (p130), which fitted with those of human MYPT1 as assessed by mass spectrometry, are shown in bold red. (For interpretation of the references to color in this figure legend, the reader is referred to the web version of this article.)

(Fig. 2A). In the control lane, neither NUAK2 nor p130 could be detected, suggesting that p130 was a NUAK2-binding substrate.

Purification of NUAK2 substrate

To characterize p130, we applied the Flag eluate to a reverse phase column. There were two radioactive peaks (fraction numbers 32–34, 42–44) detected in these fractions (Fig. 2B, upper panel) and each fraction was electrophoresed followed by autoradiography (Fig. 2B, middle panel). NUAK2 and p130 were well separated and matched to radioactive peak. To identify p130, we scaled up the purification procedure using HEK293T cells (4.0×10^7) expressing Flag-tagged NUAK2 without radioactive material. The purified products of the protein complex were resolved by SDS–PAGE and silver stained. Silver staining of these fractions detected NUAK2 and p130 (Fig. 2B, lower panel). We analyzed the peptides digested from the p130 band by mass spectrometry. P130 included fragments of the amino acid sequences of WIGSETDLEPPVVKR, QWLNSGHINDVR and LAYVAPTIPR that matched human myosin phosphatase targeting subunit 1 (MYPT1) (Fig. 2C).

MYPT1 is associated with NUAK2

To test whether MYPT1 is associated with NUAK2, HEK293T cells were transiently transfected with or without Myc-NUAK2. Protein extracts were subjected to immunoprecipitation with anti-Myc antibody, followed by immunoblotting with anti-MYPT1 antibody. We confirmed direct binding of endogenous MYPT1 to recombinant NUAK2 (Fig. 3A). Next, to identify the binding site on MYPT1 for NUAK2, we constructed several MYPT1 deletion mutants (Fig. 3B). Mutation analysis revealed that the NUAK2-binding domain corresponded to the C-terminal domain (amino acids 800–1020) of MYPT1 (Fig. 3C).

In vitro phosphorylation of MYPT1 by NUAK2

Recombinant human NUAK2 purified by baculovirus expression system efficiently phosphorylated *E. coli* recombinant MYPT1, suggesting that NUAK2 directly phosphorylates MYPT1 (Fig. 4A). Rho-kinase (ROCK) is

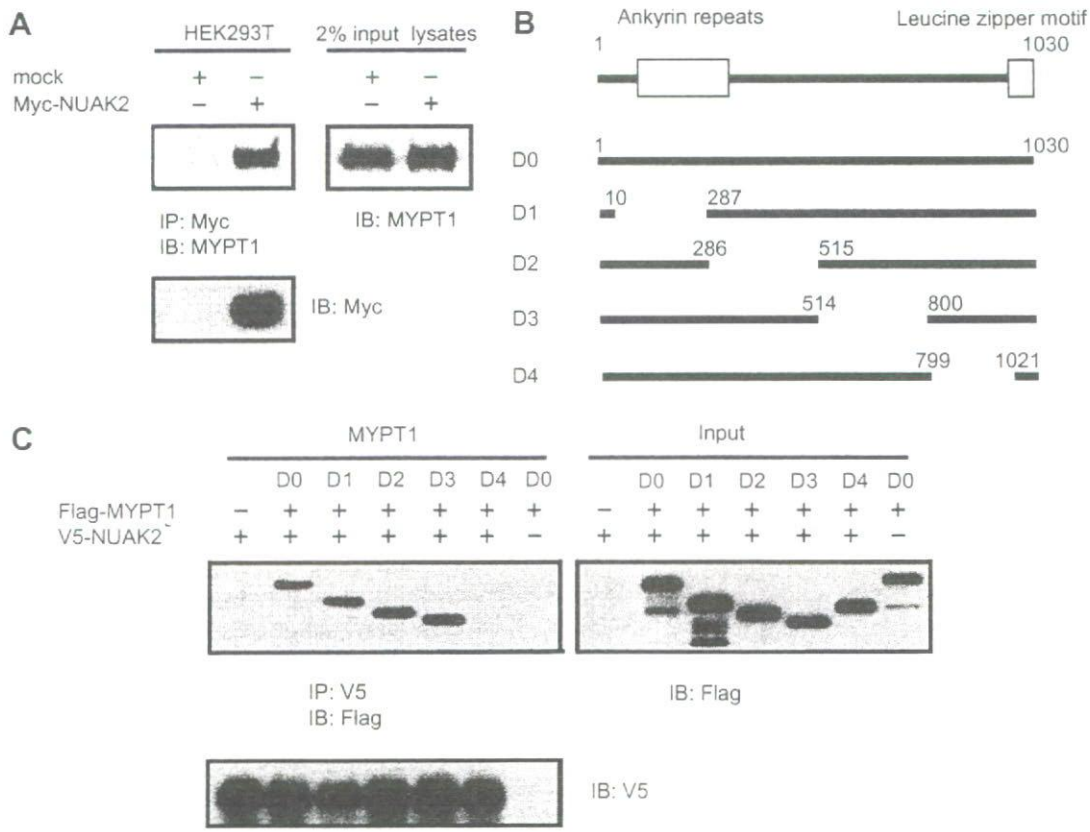

Fig. 3. NUAK2 interacts with MYPT1. (A) HEK293T cells were transiently transfected with mock or Myc-tagged NUAK2. Whole-cell extracts were ubjected to immunoprecipitation assays using anti-Myc antibody followed by immunoblotting using anti-MYPT1 antibody. The same filter was reprobed ith anti-Myc antibody. The same lysates were also analyzed by immunoblotting using anti-MYPT1 antibody. (B) Schematic model of the MYPT1 eletion mutants. The numbers are the amino acid number. (C) HEK293T cells were transiently transfected with V5-tagged NUAK2, Flag-tagged WT or arious truncated MYPT1, alone, or together as indicated. Co-immunoprecipitation assays were performed with whole-cell extracts using anti-V5 ntibody, followed by immunoblotting using anti-V5 or anti-Flag antibodies. The same lysates were also analyzed by immunoblotting using anti-Flag ntibody.

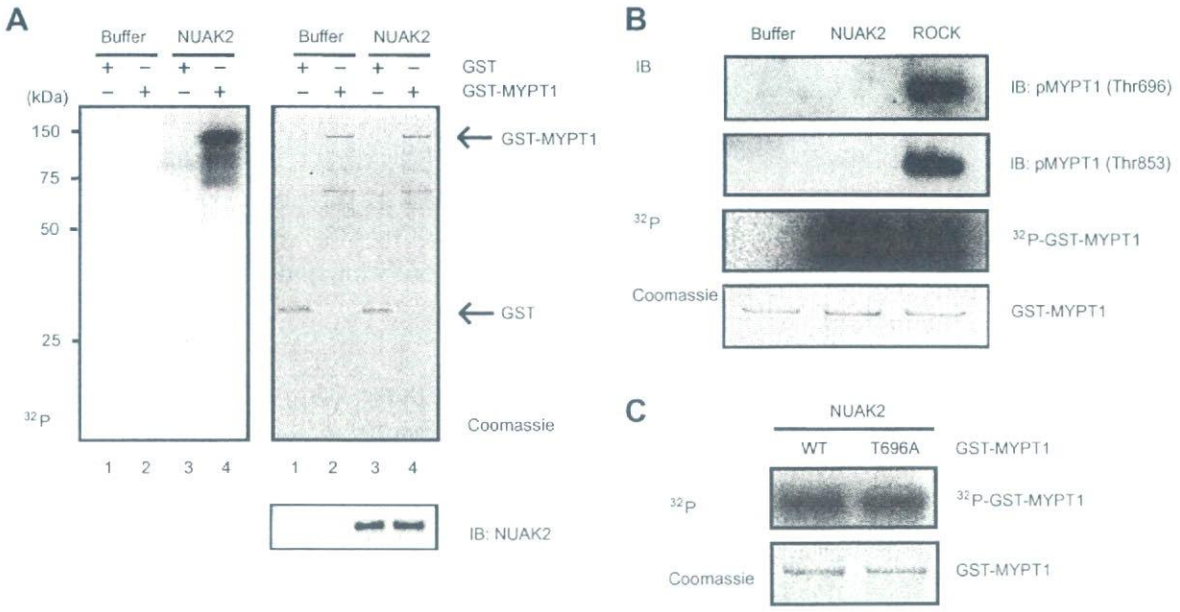

Fig. 4. NUAK2 phosphorylates MYPT1 at another site(s), other than known ROCK phosphorylation sites. (A) GST-alone (lanes 1 and 3) or GST-MYPT1 (lanes 2 and 4) were subjected to an in vitro kinase assay with control (lanes 1 and 2) or GST-NUAK2 (lanes 3 and 4), followed by autoradiography (left panel); Coomassie stain of the same gel (right upper panel), or by immunoblotting with anti-NUAK2 antibody (right lower panel). (B) GST-MYPT1 phosphorylated by recombinant NUAK2 or ROCK was resolved by SDS–PAGE followed by immunoblotting with anti-phosphospecific antibodies against MYPT1 (Thr696 or Thr853), or by autoradiography, or by Coomassie stain, as indicated. These results are representative of three independent experiments. (C) WT or the T696A mutant form of GST-MYPT1 phosphorylated by GST-NUAK2 was resolved by SDS–PAGE followed by autoradiography (upper panel); Coomassie stain of the same gel (lower panel).

known to the major kinase responsible for phosphorylation of MYPT1 [8]. To investigate how the MYPT1 phosphorylation by NUAK2 was regulated, we compared MYPT1 phosphorylation by NUAK2 and that by ROCK. ROCK is known to phosphorylate Thr696 and Thr853 in MYPT1. ROCK phosphorylated MYPT1 at the Thr696 and Thr853, confirmed by immunoblotting with anti-phospho-specific antibodies. Surprisingly, however, NUAK2 did not enhance the phosphorylation of either Thr696 or Thr853 (Fig. 4B). The non-phosphorylatable T696A mutant MYPT1 in which Thr696 was replaced with Ala was phosphorylated by NUAK2 to the same extent as WT-MYPT1 (Fig. 4C). Similarly, the T853A mutant MYPT1 also was phosphorylated by NUAK2 to the same extent as WT-MYPT1 (data not shown). These data suggests that NUAK2 phosphorylates MYPT1 at another site(s), other than known ROCK phosphorylation sites.

Discussion

TNFα is a pleiotropic cytokine that mediates diverse biological responses. To investigate the signal transduction pathways modulated by TNFα and their effect on endothelial cells, the profiles of mRNA expression extracted from HUVECs were analyzed. Most of TNFα-induced genes were chemokine family molecules and chemokine related molecules. We focused on one kinase, NUAK2 among them because it was strongly induced by TNFα. However, none of its substrate has been reported. Knowledge of kinase-substrate relationships is essential to dissect the signaling and regulatory events in which each kinase participates [9]. Direct binding of kinase to its substrate is often reported. Structural analysis reveals that the several binding sites besides catalytic site exist between kinase and its substrate [10]. The kinetics of reactions needs to be enhanced by binding between substrate and kinase. Those affinities might help efficient purification of substrate for target kinase. We successfully purified MYPT1 as a novel substrate for NUAK2 with simple two-step purification. This method is useful for rapid identification of an unknown substrate for certain kinase and can be applied for other substrate screening of kinases.

MYPT1 is a regulatory subunit of myosin phosphatase (MP) which catalyzes dephosphorylation of MLC. Phosphorylation of myosin light chain (MLC) elicits many cellular functions, including smooth muscle contraction [11,12]. MP activity is known to be regulated by upstream kinases. ROCK is most intensively examined [8]. ROCK directly binds MYPT1 and phosphorylates Thr696 and Thr853 of MYPT1 [13]. Phosphorylated MYPT1 by ROCK reduced MP activity resulting increased phosphorylation of MLC [14]. Several other kinases (MYPT1 kinase, integrin-linked kinase and myotonic dystrophy protein kinase) also can phosphorylate the same inhibitory site (Thr696) on MYPT1 [15–17]. The mechanism to reduce MP activity by MYPT1 phosphorylation is still unknown, however, phosphorylation of Thr853 was suggested to directly reduce MYPT1 binding to myosin [18]. Dissociation of the MP holoenzyme by MYPT1 phosphorylation is another suggested mechanism of reduced MYPT1 activ-

ity [19]. NUAK2 did not phosphorylate MYPT1 at either Thr696 or Thr853, confirmed by immunoblotting with anti-phosphospecific antibodies (Fig. 4B) and mutation analysis of MYPT1 (Fig. 4C). These data suggest that NUAK2 phosphorylates MYPT1 at a different site(s) to elicit different regulatory functions. Further characterization of phosphorylation site(s) and elucidation of MYPT1 regulation by NUAK2 are necessary for future study.

Physiological function has been seldom analyzed about NUAK2, however, Legembre et al. reported that NUAK2 works as a part of antiapoptotic signals and an enhancer of cell mobility [4]. If NUAK2 phosphorylates MYPT1 and modulates MLC phosphorylation, these phenotypes would be explained by functional regulation of MYPT1 and its target molecule, myosin. One intriguing thing about NUAK2 is that this is the only kinase highly induced by TNFα. Most of other induced genes were chemokines and adhesion molecules. Chemokine induces chemotaxis of various normal cells, and also plays an important role for invasiveness of tumor cells partly reflected by cell motility. NUAK2-mediated MYPT1 phosphorylation might enhance these chemokine signaling by modifying myosin motor function. In tumor cell lines, TNFα also strongly induces expression of NUAK2, which is related to its motility and invasiveness [4]. These tumor characteristics might be also regulated by NUAK2-mediated myosin motor regulation. The physiological significance of the phosphorylation of MYPT1 by NUAK2 both in normal cells and in tumor cells is now under investigation.

Acknowledgments

We thank A. Ogai, H.O. kuda, S. Ikezawa and Y. Hamada for technical assistance. We thank Dr. M. Ito for thoughtful discussion. This study was supported by a Grant from Japan Cardiovascular Research Foundation. Supported by Grants-in-aid for Human Genome, Tissue Engineering, and Food Biotechnology (H13-Genome-011) in Health and Labor Sciences Research Grants Research, Comprehensive Research on Aging and Health (H13-21 seiki (seikatsu)-23) in Health and Labor Sciences Research Grants Research from Ministry of Health and Labor and Welfare, Takeda Science Foundation and Grant-in-aid for Scientific Research (No. 17390229) from the Ministry of Education, Science, and Culture, Japan.

References

[1] T. Collins, M.A. Read, A.S. Neish, M.Z. Whitley, D. Thanos, T. Maniatis, Transcriptional regulation of endothelial cell adhesion molecules: NF-kappa B and cytokine-inducible enhancers, FASEB J. 9 (1995) 899–909.

[2] D.L. Lefebvre, Y. Bai, N. Shahmolky, M. Sharma, R. Poon, D.J. Drucker, C.F. Rosen, Identification and characterization of a novel sucrose-non-fermenting protein kinase/AMP-activated protein kinase-related protein kinase, SNARK, Biochem. J. 355 (2001) 297–305.

[3] D.L. Lefebvre, C.F. Rosen, Regulation of SNARK activity in response to cellular stresses, Biochim. Biophys. Acta 1724 (2005) 71–85.

[4] P. Legembre, R. Schickel, B.C. Barnhart, M.E. Peter, Identification of SNF1/AMP kinase-related kinase as an NF-kappaB-regulated anti-apoptotic kinase involved in CD95-induced motility and invasiveness, J. Biol. Chem. 279 (2004) 46742–46747.

[5] Y. Asano, S. Takashima, M. Asakura, Y. Shintani, Y. Liao, T. Minamino, H. Asanuma, S. Sanada, J. Kim, A. Ogai, T. Fukushima, Y. Oikawa, Y. Okazaki, Y. Kaneda, M. Sato, J. Miyazaki, S. Kitamura, H. Tomoike, M. Kitakaze, M. Hori, Lamr1 functional retroposon causes right ventricular dysplasia in mice, Nat. Genet. 36 (2004) 123–130.

[6] S. Soker, S. Takashima, H.Q. Miao, G. Neufeld, M. Klagsbrun, Neuropilin-1 is expressed by endothelial and tumor cells as an isoform-specific receptor for vascular endothelial growth factor, Cell 92 (1998) 735–745.

[7] T. Minamino, V. Gaussin, F.J. DeMayo, M.D. Schneider, Inducible gene targeting in postnatal myocardium by cardiac-specific expression of a hormone-activated Cre fusion protein, Circ. Res. 88 (2001) 587–592.

[8] K. Kimura, M. Ito, M. Amano, K. Chihara, Y. Fukata, M. Nakafuku, B. Yamamori, J. Feng, T. Nakano, K. Okawa, A. Iwamatsu, K. Kaibuchi, Regulation of myosin phosphatase by Rho and Rho-associated kinase (Rho-kinase), Science 273 (1996) 245–248.

[9] D.C. Berwick, J.M. Tavare, Identifying protein kinase substrates: hunting for the organ-grinder's monkeys, Trends Biochem. Sci. 29 (2004) 227–232.

[10] C. Kim, N.H. Xuong, S.S. Taylor, Crystal structure of a complex between the catalytic and regulatory (RIalpha) subunits of PKA, Science 307 (2005) 690–696.

[11] F. Matsumura, Regulation of myosin II during cytokinesis in higher eukaryotes, Trends Cell Biol. 15 (2005) 371–377.

[12] M. Ito, T. Nakano, F. Erdodi, D.J. Hartshorne, Myosin phosphatase: structure, regulation and function, Mol. Cell Biochem. 259 (2004) 197–209.

[13] D. Johnson, P. Cohen, M.X. Chen, Y.H. Chen, P.T. Cohen, Identification of the regions on the M110 subunit of protein phosphatase 1 M that interact with the M21 subunit and with myosin, Eur. J. Biochem. 244 (1997) 931–939.

[14] J. Feng, M. Ito, K. Ichikawa, N. Isaka, M. Nishikawa, D.J. Hartshorne, T. Nakano, Inhibitory phosphorylation site for Rho-associated kinase on smooth muscle myosin phosphatase, J. Biol. Chem. 274 (1999) 37385–37390.

[15] J.A. MacDonald, M.A. Borman, A. Muranyi, A.V. Somlyo, D.J. Hartshorne, T.A. Haystead, Identification of the endogenous smooth muscle myosin phosphatase-associated kinase, Proc. Natl. Acad. Sci. USA 98 (2001) 2419–2424.

[16] A. Muranyi, J.A. MacDonald, J.T. Deng, D.P. Wilson, T.A. Haystead, M.P. Walsh, F. Erdodi, E. Kiss, Y. Wu, D.J. Hartshorne, Phosphorylation of the myosin phosphatase target subunit by integrin-linked kinase, Biochem. J. 366 (2002) 211–216.

[17] A. Muranyi, R. Zhang, F. Liu, K. Hirano, M. Ito, H.F. Epstein, D.J. Hartshorne, Myotonic dystrophy protein kinase phosphorylates the myosin phosphatase targeting subunit and inhibits myosin phosphatase activity, FEBS Lett. 493 (2001) 80–84.

[18] G. Velasco, C. Armstrong, N. Morrice, S. Frame, P. Cohen, Phosphorylation of the regulatory subunit of smooth muscle protein phosphatase 1 M at Thr850 induces its dissociation from myosin, FEBS Lett. 527 (2002) 101–104.

[19] J. Tanaka, M. Ito, J. Feng, K. Ichikawa, T. Hamaguchi, M. Nakamura, D.J. Hartshorne, T. Nakano, Interaction of myosin phosphatase target subunit 1 with the catalytic subunit of type 1 protein phosphatase, Biochemistry 37 (1998) 16697–16703.

Human atrial natriuretic peptide and nicorandil as adjuncts to reperfusion treatment for acute myocardial infarction (J-WIND): two randomised trials

*Masafumi Kitakaze, Masanori Asakura, Jiyoong Kim, Yasunori Shintani, Hiroshi Asanuma, Toshimitsu Hamasaki, Osamu Seguchi, Masafumi Myoishi, Tetsuo Minamino, Takahiro Ohara, Yoshiyuki Nagai, Shinsuke Nanto, Kouki Watanabe, Shigeru Fukuzawa, Atsushi Hirayama, Natsuki Nakamura, Kazuo Kimura, Kenshi Fujii, Masaharu Ishihara, Yoshihiko Saito, Hitonobu Tomoike, Soichiro Kitamura, and the J-WIND investigators**

Summary

Background Patients who have acute myocardial infarction remain at major risk of cardiovascular events. We aimed to assess the effects of either human atrial natriuretic peptide or nicorandil on infarct size and cardiovascular outcome.

Methods We enrolled 1216 patients who had acute myocardial infarction and were undergoing reperfusion treatment in two prospective, single-blind trials at 65 hospitals in Japan. We randomly assigned 277 patients to receive intravenous atrial natriuretic peptide (0·025 μg/kg per min for 3 days) and 292 the same dose of placebo. 276 patients were assigned to receive intravenous nicorandil (0·067 mg/kg as a bolus, followed by 1·67 μg/kg per min as a 24-h continuous infusion), and 269 the same dose of placebo. Median follow-up was 2·7 (IQR 1·5–3·6) years for patients in the atrial natriuretic peptide trial and 2·5 (1·5–3·7) years for those in the nicorandil trial. Primary endpoints were infarct size (estimated from creatine kinase) and left ventricular ejection fraction (gauged by angiography of the left ventricle).

Findings 43 patients withdrew consent after randomisation, and 59 did not have acute myocardial infarction. We did not assess infarct size in 50 patients for whom we had fewer than six samples of blood. We did not have angiographs of left ventricles in 383 patients. Total creatine kinase was 66 459·9 IU/mL per h in patients given atrial natriuretic peptide, compared with 77 878·9 IU/mL per h in controls, with a ratio of 0·85 between these groups (95% CI 0·75–0·97, p=0·016), which indicated a reduction of 14·7% in infarct size (95% CI 3·0–24·9%). The left ventricular ejection fraction at 6–12 months increased in the atrial natriuretic peptide group (ratio 1·05, 95% CI 1·01–1·10, p=0·024). Total activity of creatine kinase did not differ between patients given nicorandil (70 520·5 IU/mL per h) and controls (70 852·7 IU/mL per h) (ratio 0·995, 95% CI 0·878–1·138, p=0·94). Intravenous nicorandil did not affect the size of the left ventricular ejection fraction, although oral administration of nicorandil during follow-up increased the left ventricular ejection fraction between the chronic and acute phases. 29 patients in the atrial natriuretic peptide group had severe hypotension, compared with one in the corresponding placebo group.

Interpretation Patients with acute myocardial infarction who were given atrial natriuretic peptide had lower infarct size, fewer reperfusion injuries, and better outcomes than controls. We believe that atrial natriuretic peptide could be a safe and effective adjunctive treatment in patients with acute myocardial infarction who receive percutaneous coronary intervention.

Lancet 2007; 370: 1483–93

See **Comment** page 1461

*Other investigators listed at end of study

Cardiovascular Division of Medicine, National Cardiovascular Centre, Suita, Osaka, Japan (Prof M Kitakaze MD, M Asakura MD, J Kim MD, O Seguchi MD, M Myoishi MD, T Ohara MD, Prof H Tomoike MD, Prof S Kitamura MD); **Department of Clinical Research and Development, National Cardiovascular Centre, Suita, Osaka, Japan** (M Kitakaze MD, M Asakura MD); **Department of Internal Medicine and Therapeutics, Osaka University Graduate School of Medicine, Suita, Osaka, Japan** (Y Shintani MD, T Minamino MD); **Research Institute, National Cardiovascular Centre, Suita, Osaka, Japan** (H Asanuma MD); **Department of Biomedical Statistics, Osaka University Graduate School of Medicine, Suita, Osaka, Japan** (T Hamasaki PhD); **Heart Centre Department of Cardiology, Rinku General Medical Centre, Izumisano, Osaka, Japan** (Y Nagai MD); **Cardiovascular Division, Kansai Rosai Hospital, Amagasaki, Hyogo, Japan** (Prof S Nanto MD); **Department of Cardiology, Uwajima-City Hospital, Uwajima, Ehime, Japan** (K Watanabe MD); **Division of Cardiology, Funabashi Municipal Medical Centre, Funabashi, Chiba, Japan** (S Fukuzawa MD); **Cardiovascular Division, Osaka Police Hospital, Osaka, Osaka, Japan** (Prof A Hirayama MD); **Department of Cardiology, Shinbeppu Hospital, Beppu, Oita, Japan** (N Nakamura MD); **Division of Cardiology, Yokohama City University Medical Centre, Yokohama,**

Introduction

Despite availability of effective medical treatments, chronic heart failure remains a major cause of morbidity and mortality worldwide.[1–3] Ischaemic heart disease, in turn, is one of the main causes of chronic heart failure.[4] The most important treatment objectives are prevention of acute myocardial infarction, and, in individuals who have an acute myocardial infarction, reduction in infarct size and ischaemia or reperfusion injury.[5] Only a few medications have been shown to decrease ischaemia or reperfusion injury.[6–8]

Reperfusion of ischaemic myocardium reduces infarct size and improves left ventricular function, both of which contribute to better clinical outcomes in patients with acute myocardial infarction.[9–11] However, reperfusion can also cause tissue damage.[12] Several drugs have been trialled for the prevention or amelioration of such injuries, but results have not been consistently satisfactory.[13–15] Recently, human atrial natriuretic peptide and nicorandil have both been shown to be effective for reduction of myocardial damage after acute myocardial infarction in basic and clinical studies.[16–25] Atrial natriuretic peptide is a candidate for adjunctive treatment after acute myocardial infarction, because it has been shown to suppress the renin–angiotensin–aldosterone system and endothelin-1, both of which which modulate infarct size and cardiac remodelling.[19] Nicorandil is a combined adenosine triphosphate (ATP)-sensitive potassium channel opener and nitrate preparation that has also shown promise as an adjunctive treatment for acute myocardial infarction. In the clinical setting, however,

Kanagawa, Japan (Prof K Kimura MD); Division of Cardiology, Sakurabashi Watanabe Hospital, Osaka, Osaka, Japan (K Fujii MD); Department of Cardiology, Hiroshima City Hospital, Hiroshima, Hiroshima, Japan (M Ishihara MD); and First Department of Medicine, Nara Medical University, Kashihara, Nara, Japan (Prof Y Saito MD)

Correspondence to: Professor Masafumi Kitakaze, Cardiovascular Division of Medicine, National Cardiovascular Centre Suita, Osaka 565-8565, Japan
kitakaze@hsp.ncvc.go.jp

the beneficial effects of atrial natriuretic peptide and nicorandil have only been tested in single-centre studies with small sample sizes.[20–25] The Japan working group studies on acute myocardial infarction for the reduction of necrotic damage by human atrial natriuretic peptide or nicorandil (J-WIND-ANP and J-WIND-KATP, respectively) aimed to assess the value of these drugs as adjuncts to percutaneous coronary intervention for patients with acute myocardial infarction.

Methods

Patients

We have described the protocols for the two trials previously.[26,27] In brief, we recruited patients to two independent, investigator-initiated, investigator-led, multicentre, prospective, randomised, single-blind, controlled trials at 65 hospitals. 27 hospitals participated in the atrial natriuretic peptide trial, and 38 separate hospitals in the nicorandil trial (table 1); the two studies were completely independent. We initially planned to include fewer hospitals, but we increased the number to promote enrolment of sufficient patients.

Eligibility criteria were age between 20 and 79 years; chest pain for more than 30 min; at least 0·1 mV of ST segment elevation in two adjacent ECG leads; admission to hospital within 12 h of the onset of symptoms; and one instance of acute myocardial infarction. Exclusion criteria were a history of myocardial infarction; left main trunk stenosis; severe liver or kidney dysfunction or both; suspected aortic dissection; previous coronary artery bypass grafting; and a history of drug allergy.

All patients gave written informed consent immediately after admission to hospital, and were asked to sign the same consent form again after 2 weeks when they had more time to decide. This system was applied on the recommendation of the institutional review boards. Only one patient, who was in the nicorandil group, withdrew their consent at their second opportunity. We enrolled patients from Oct 24, 2001, to Dec 13, 2005. The study protocol was approved by the institutional review boards and ethics committees of all participating hospitals, and was in accordance with the Declaration of Helsinki.

Procedures

An independent statistician generated our randomisation lists with a computer, by the permuted-block method. Within each centre, the block length was eight. Treatment allocations were concealed in opaque sealed envelopes until patients were enrolled. Physicians were not aware of the random assignments of patients until the follow-up stage; patients and those who analysed the data were unaware of the treatment assignment for the duration of the study. Both trials were designed as single-blind studies.

277 patients who were enrolled in the atrial natriuretic peptide trial were randomly assigned to receive an intravenous infusion of this drug after reperfusion treatment, at 0·025 μg/kg per min for 3 days, and 292 a placebo of 5% glucose solution by the same method. 276 patients in the other trial were randomly assigned to intravenous nicorandil, infused at 1·67 μg/kg per min for 24 h after bolus injection of nicorandil at a dose of 0·067 mg/kg, and 269 were assigned to 0·9% saline solution, by the same method. Previous studies have shown substantial cardiovascular protection with atrial natriuretic peptide and nicorandil at these doses.[20,22] Of the 276 patients assigned to receive nicorandil, 61 were given nicorandil orally, at the discretion of individual investigators, during the follow-up period.

We planned to stop the administration of treatment drugs in case of severe hypotension, which was defined as systolic blood pressure of less than 90 mm Hg, because of the vasodilator effect of these drugs. The study protocol did not restrict or specify any other diagnostic or therapeutic methods in the acute phase (2–8 weeks after acute myocardial infarction) or chronic phase (6–12 months).

We obtained data on baseline characteristics, emergent catheterisation, and medication at discharge after 1 month; data on follow-up catheterisation and medication after 6 months; and data on medication after 24 months. We also followed up all patients for cardiovascular events (ie, cardiac death, readmission to hospital due to heart failure, new onset of acute coronary syndrome, or revascularisation of new lesions) until the end of August, 2006. We took blood samples to measure concentrations of creatine kinase at a central laboratory, before the procedure and at 1, 3, 6, 9, 12, 18, 24, 36, 48, and 72 h after the onset of reperfusion.[14] We analysed total creatine kinase for all patients with at least six blood samples. We obtained right anterior oblique views with angiography of the left ventricle once in the acute phase (2–8 weeks), and once in the chronic phase (6–12 months).

Our primary endpoints were infarct size (which was estimated as the area under the concentration versus time curve for creatine kinase)[14] and ventricular ejection fraction (which was assessed by angiography of the left ventricle at 6–12 months after hospital admission).[15] The prespecified secondary endpoints were survival rate; cardiovascular events (such as cardiac death, readmission to hospital for heart failure, new onset of acute coronary syndrome, or revascularisation of new lesions); incidence of cardiac death or readmission to hospital for

	J-WIND-ANP study	J-WIND-KATP study
1–4 patients	7 hospitals	9 hospitals
5–9 patients	3 hospitals	13 hospitals
10–19 patients	7 hospitals	6 hospitals
More than 20 patients	10 hospitals	10 hospitals

Table 1: **Distribution of patients between participating hospitals**

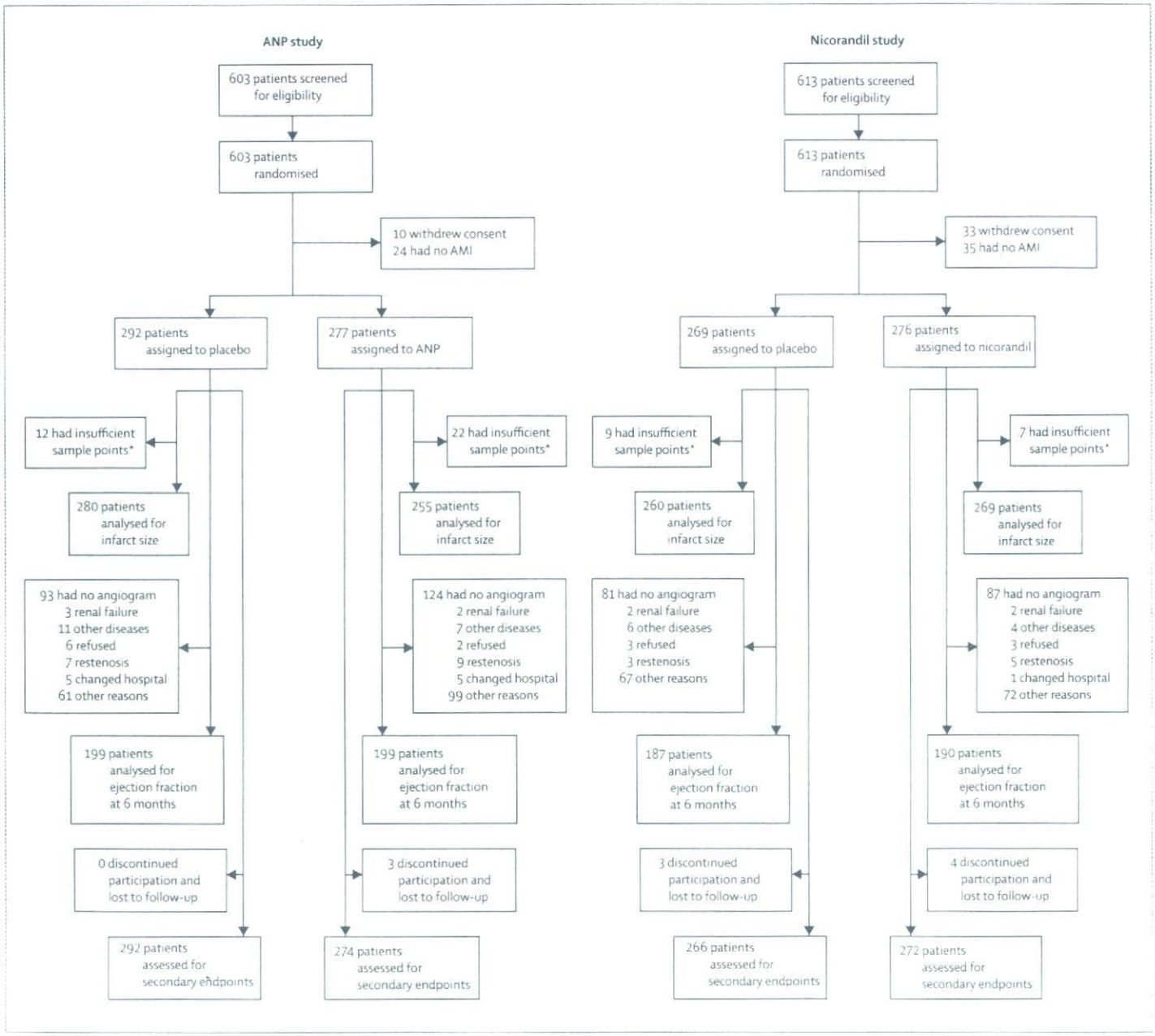

Figure 1: **Trial profiles**
ANP=atrial natriuretic peptide. AMI=acute myocardial infarction. *Fewer than six blood samples.

heart failure; or reperfusion injury before discharge from coronary care unit (such as malignant ventricular arrhythmia during reperfusion, recurrence of ST segment elevation, or worsening of chest pain). We also assessed infarct size, estimated by peak creatine kinase and troponin T;[28,29] left ventricular ejection fraction at acute phase; and end-diastolic or end-systolic volume index (assessed by angiography of the left ventricle). We looked at the effects of each drug on the primary endpoints in prespecified subgroups (sex, age, body-mass index, pre-angina, elapsed time between acute myocardial infarction and intervention, diabetes mellitus, hyperlipidaemia, smoking, and family history of acute myocardial infarction). We also did post-hoc analyses on the effect of chronic administration of nicorandil on the ejection fraction.

All data were collected by Koteisho-kyokai (Tokyo), an organisation established by the Japanese government in 2001–2003 and by NTT Data (Tokyo) in 2004–2006. Left ventricular ejection fraction and end-diastolic volume were measured by the area–length method, from angiography of the left ventricle. Two independent

interpreters, who were unaware of the treatment assigned to patients, measured left ventricular ejection fractions from the angiographs. We calculated the average value, unless the two investigators disagreed, in which case we referred to a third opinion.

Clinical findings and medications during the follow-up period were reported to a data and safety committee after registration. This committee, which consisted of three physicians and one statistician who did not participate in the trial, monitored all adverse events. Research nurses or doctors visited all participating hospitals to check that patients were registered, drugs were given, and data collected according to the protocol. Committee members did not provide any results to the steering committee, because discontinuation of the study was not recommended.

Statistical analysis

We calculated that a sample size of 300 patients would be needed in each group to detect a 20% reduction in the most important primary endpoint (total creatine kinase) with a statistical power of 80% at significance level of 0·05 (with a two-sided *t* test), accounting for dropout of some patients. We set equal sample sizes in both groups, because we expected to see almost the same reduction in infarct size with either treatment. Since creatine kinase and total creatine kinase are both log-normally distributed,[30] total creatine kinase was log-transformed before analysis. The left ventricular ejection fraction was also log-transformed before the analysis since the distribution was skewed.

Statistical analysis was done according to a prespecified analytical plan. Efficacy analysis was based on intention to treat. The primary efficacy analyses for total creatine kinase and left ventricular ejection fraction were done simply by *t* test. The estimated mean and differences on the log scale were transformed back to the original scale and were expressed as geometric means and ratios of geometric mean. If the calculated 95% CI for the ratio of the geometric mean did not cross the point of no effect (ie, 1) the difference between groups was regarded as significant. Furthermore, analysis of covariance for the two endpoints was used to estimate adjusted mean comparison, with effect of covariates and the interactions. We imputed missing data for patients by the predicted mean imputation method, with nonlinear regression. We applied multiple imputation techniques (with group means, Markov Chain Monte Carlo, Bayesian bootstrap, and last-observation-carried-forward methods) to assess the robustness and sensitivity of our conclusions.

Proportions were examined by Fisher's exact test. We examined time-to-event by the Kaplan-Meier method to estimate the survival for each group and then the differences in survival between groups by the log-rank test. The Cox proportional hazards model was used to assess baseline risk factors and an adjusted hazard ratio. The proportional hazards assumption was investigated graphically, with a test based on Schoenfeld residuals.[31,32]

All tests were two-sided, and a p value of less than 0·05 was regarded as significant. All analyses were done with SAS software (version 8.2). The trials are registered with Clinicaltrials.gov, numbers NCT00212056 and NCT00212030.

Role of the funding source

The sponsors of the study had no role in study design, data collection, data analysis, data interpretation, or writing of the report. The corresponding author had full access to all data at the end of the study, and had final responsibility for the decision to submit for publication.

Results

Figure 1 shows the trial profile. Table 2 shows baseline characteristics. Median follow-up was 2·7 (IQR 1·5–3·6) years in the atrial natriuretic peptide trial and 2·5 (1·5–3·7) years in the nicorandil trial. Table 3 shows

	Atrial natriuretic peptide study			Nicorandil study		
	ANP (n=277)	Control (n=292)	p	Nicorandil (n=276)	Control (n=269)	p
Age (years)	63·0 (10·4)	61·8 (10·7)	0·1652	61·1 (11·4)	63·7 (10·2)	0·0035
Sex (male)	211 (76·2%)	243 (83·2%)	0·0374	246 (89·1%)	220 (81·8%)	0·0153
Body-mass index	24·3 (3·5)	24·0 (2·9)	0·3733	24·2 (3·0)	23·4 (2·8)	0·0007
Killip classification (I, II, III, IV)	88·6%, 9·5%, 1·1%, 0·8%	90·3%, 7·5%, 1·4%, 0·7%	0·5274	91·1%, 8·2%, 0·4%, 0·4%	92·0%, 4·2%, 2·7%, 1·1%	0·7843
Pre-angina	105 (44·5%)	118 (46·1%)	0·7862	111 (44·6%)	111 (43·9%)	0·9284
Risk factors						
Hypertension	137 (56·1%)	162 (62·1%)	0·2046	127 (48·5%)	137 (53·9%)	0·2190
Diabetes mellitus	81 (33·8%)	86 (33·9%)	1·0000	104 (39·5%)	82 (32·9%)	0·1413
Hyperlipidaemia	127 (54·3%)	131 (50·6%)	0·4181	121 (46·7%)	114 (46·2%)	0·9291
Smoking	158 (63·7%)	175 (67·3%)	0·4022	178 (68·7%)	170 (66·1%)	0·5732

Data are number (%) or mean (SD), unless otherwise specified. ANP=atrial natriuretic peptide.

Table 2: **Baseline characteristics on admission**

	Atrial natriuretic peptide study		Nicorandil study	
	ANP (n=277)	Control (n=292)	Nicorandil (n=276)	Control (n=269)
Elapsed time (h)*	4·00 (3·00–6·00)	4·00 (2·50–6·00)	3·50 (2·50–5·00)	3·50 (2·50–5·00)
Infusion time (h)	1·00 (0·50–1·00)	1·00 (0·50–1·00)	0·70 (0·50–1·00)	0·75 (0·50–1·00)
IRA (LAD, LCx, RCA)	55·3%, 6·4%, 38·3%	52·3, 10·6, 37·1%	53·9, 7·4, 38·7%	44·5, 9·9, 45·6%
Stents	176 (63·5%)	193 (66·1%)	187 (67·8%)	183 (68·0%)
Rescue	64 (23·1%)	92 (31·5%)	94 (34·1%)	92 (34·2%)
Intra-aortic balloon pump	17 (6·1%)	14 (4·8%)	14 (5·1%)	15 (5·6%)
Final stenosis (<75%)	246 (93·5%)	266 (94·7%)	257 (96·6%)	255 (97·0%)
Final thrombolysis in myocardial infarction (0, 1, 2, 3)	3·9%, 1·9%, 5·0%, 89·1%	5·2%, 0·7%, 4·1%, 90·0%	3·7%, 0·7%, 5·2%, 90·3%	3·4%, 1·1%, 6·9%, 88·5%
Medications at 1 month				
ACE inhibitor	155 (57·8%)	173 (60·7%)	164 (61·0%)	163 (62·0%)
ARB	77 (28·7%)	99 (34·7%)	72 (26·8%)	69 (26·2%)
Spinorolactone	28 (10·4%)	33 (11·6%)	17 (6·3%)	22 (8·4%)
β blocker	112 (41·8%)	128 (44·9%)	110 (40·9%)	121 (46·0%)
Aspirin	225 (84·0%)	252 (88·4%)	251 (93·3%)	250 (95·1%)
Nitrates	81 (30·2%)	86 (30·2%)	50 (18·6%)	63 (24·0%)
Statins	129 (48·1%)	156 (54·7%)	126 (46·8%)	115 (43·7%)
Nicorandil	62 (23·1%)	52 (18·2%)	79 (29·4%)	34 (12·9%)
Medications at 6 months				
ACE inhibitor	103 (48·1%)	117 (44·8%)	120 (50·6%)	131 (53·9%)
ARB	69 (32·2%)	110 (42·1%)	68 (28·7%)	75 (30·9%)
Spinorolactone	26 (12·1%)	26 (10·0%)	11 (4·6%)	15 (6·2%)
β blocker	93 (43·5%)	118 (45·2%)	104 (43·9%)	113 (46·5%)
Aspirin	179 (83·6%)	233 (89·3%)	217 (91·6%)	229 (94·2%)
Nitrates	51 (23·8%)	63 (24·1%)	37 (15·6%)	49 (20·2%)
Statins	112 (52·3%)	150 (57·5%)	123 (51·9%)	118 (48·6%)
Nicorandil	46 (21·5%)	39 (14·9%)	55 (23·2%)	23 (9·5%)
Medications at 24 months				
ACE inhibitor	66 (47·5%)	63 (37·5%)	83 (52·5%)	75 (49·3%)
ARB	42 (30·2%)	72 (42·9%)	39 (24·7%)	43 (28·3%)
Spinorolactone	13 (9·4%)	21 (12·5%)	9 (5·7%)	4 (2·6%)
β blocker	57 (41·0%)	61 (36·3%)	77 (48·7%)	71 (46·7%)
Aspirin	113 (81·3%)	133 (79·2%)	143 (90·5%)	137 (90·1%)
Nitrates	29 (20·9%)	45 (26·8%)	23 (14·6%)	25 (16·4%)
Statins	66 (47·5%)	78 (46·4%)	81 (51·3%)	71 (46·7%)
Nicorandil	26 (18·7%)	26 (15·5%)	28 (17·7%)	11 (7·2%)

Data are median (IQR), number (%) or mean (SD), unless otherwise specified. ANP=atrial natriuretic peptide. IRA=infarct-related artery. LAD=left anterior descending coronary artery. LCx=left circumflex artery. RCA=right coronary artery. ARB=antiotensin receptor blocker. ACE=angiotensin-converting enzyme. *Period between acute myocardial infarction and start of intervention.

Table 3: **Treatments and prescribed drugs**

treatments and drugs throughout the study. Drugs used in the chronic stage did not differ between groups in either study, except that some patients in the nicorandil trial were given oral nicorandil during follow-up.

Table 4 and figure 2 show infarct size and left ventricular function at 2–8 weeks and 6–12 months in both studies. The ratio of total creatine kinase between the atrial natriuretic peptide and placebo groups was 0·85 (95% CI 0·75–0·97, p=0·0155); which indicates that atrial natriuretic peptide was associated with a reduction of 14·7% in infarct size. Subanalyses identified no factors that enhanced or reduced the influence of atrial natriuretic peptide on infarct size (figure 2). Nicorandil did not reduce infarct size compared with placebo, and no factors affected this finding. Treatment with atrial natriuretic peptide tended to increase the left ventricular ejection fraction (ratio 1·043, 95% CI 1·000–1·089, p=0·0525) at 2–8 weeks after the onset of acute myocardial infarction, and at 6–12 months (ratio 1·051, 95% CI 1·006–1·099, p=0·0236). By contrast, table 4 and figure 2 show that left ventricular ejection fraction did not differ in patients given nicorandil and controls at either 2–8 weeks or 6–12 months.

	J-WIND-ANP study			J-WIND-KATP study		
	Atrial natriuretic peptide	Control	p	Nicorandil	Control	p
Infarct size						
n	255	280		269	260	
Creatine kinase (area under curve) (IU/L h)	66 459·9 (60 258·2–73 300·0)	77 878·9 (71 590·2–84 720·1)	0·016	70 520·5 (64 309·8–77 331·0)	70 852·7 (65 066·7–77 153·2)	0·941
Peak creatine kinase (IU/L)	2487·5 (2217·6–2790·3)	2784·2 (2526·7–3067·9)	0·141	2557·1 (2306·1–2835·4)	2428·7 (2199·8–2681·5)	0·479
Troponin-T concentration (12–18 h) (ng/mL)	5·36 (4·76–6·03)	6·13 (5·55–6·79)	0·084	6·18 (5·51–6·93)	5·60 (4·97–6·32)	0·244
Troponin T (96 h) (ng/mL)	2·57 (2·25–2·94)	2·94 (2·64–3·27)	0·125	2·63 (2·36–2·94)	2·89 (2·61–3·19)	0·225
Left ventricle (2–8 weeks)						
n	187	207		168	170	
Median elapsed time (days)*	18·5 (IQR 15·0–27·0)	19·0 (IQR 16·0–25·0)		17·0 (IQR 14·0–23·0)	17·0 (IQR 14·0–24·0)	
Ejection fraction	43·0% (41·8–44·3)	41·3% (40·0–42·6)	0·053	42·0% (40·7–43·3)	41·6% (40·4–42·9)	0·680
End diastolic volume index (mL/m²)	98·8 (94·4–103·4)	102·3 (98·1–106·6)	0·272	111·2 (106·4–116·3)	105·9 (100·9–111·3)	0·147
End systolic volume index (mL/m²)	54·2 (51·2–57·4)	58·3 (55·5–61·4)	0·058	62·8 (59·2–66·6)	60·4 (57·0–64·1)	0·360
Left ventricle (6–12 months)						
n	155	199		190	187	
Median elapsed time (days)*	196·5 (IQR 180·5–230·5)	200·5 (IQR 183·0–226·0)		195·0 (IQR 180·0–231·0)	195·5 (IQR 183·0–232·0)	
Ejection fraction	44·7% (43·4–46·0)	42·5% (41·2–43·9)	0·024	42·5% (41·2–43·8)	43·2% (42·0–44·4)	0·460
End diastolic volume index (mL/m²)	100·6 (95·2–106·2)	100·9 (96·8–105·1)	0·930	109·8 (105·4–114·4)	105·7 (100·8–110·8)	0·230
End systolic volume index (mL/m²)	54·2 (50·6–58·0)	56·0 (53·1–58·9)	0·452	61·7 (58·4–65·2)	58·5 (55·1–62·1)	0·198

Data are mean (95% CI) or median (IQR). *Time between acute myocardial infarction and start of intervention.

Table 4: **Primary endpoints and other outcomes obtained by angiography of left ventricles**

Figure 3 shows reperfusion injuries, survival rates, and cardiovascular events. Reperfusion injuries were less common in the atrial natriuretic peptide group than in the placebo group (ratio 0·743, 95% CI 0·58–0·952, p=0·019). Although there were no differences between groups in either survival rates or the incidence of cardiovascular events, both cardiac death and readmission to hospital for heart failure were lower in patients given atrial natriuretic peptide than in controls (HR 0·267, 95% CI 0·089–0·799, p=0·0112). By contrast, cardiac death and readmission to hospital for heart failure were not significantly lower in patients given nicorandil than in controls (HR 0·799, 95% CI 0·307–1·973, p=0·5972). When nicorandil was given orally throughout the study after reperfusion treatment, the change of left ventricular ejection fraction increased substantially between the acute and chronic phase. The ejection fraction was 3·66% in the 61 patients who were given nicorandil orally, and 1·47% in the 241 patients who were not (difference 2·20, 95% CI 0·17–4·22, p=0·0338).

In the atrial natriuretic peptide trial, 29 patients given that drug had severe hypotension during the acute phase, compared with one control. In the other trial, three patients in the nicorandil group had severe hypotension, compared with no controls. No other severe adverse events were reported during the course of either study.

Discussion

We showed that adjunctive, acute-phase treatment with atrial natriuretic peptide after reperfusion therapy in patients with acute myocardial infarction reduced infarct size by 14·7%, increased the left ventricular ejection fraction during the chronic phase, and decreased the incidence of cardiac death and readmission to hospital because of heart failure. Intravenous treatment with nicorandil did not affect the primary endpoints, although patients who were given nicorandil orally had better cardiac function outcomes.

Interest in the cardioprotective effects of adenosine has increased, because of its variety of cardioprotective mechanisms. Unfortunately, in trials of adenosine, it only marginally improved infarct size and showed no clinical benefits.[7,33] We hypothesised that treatment with atrial natriuretic peptide and nicorandil in the acute phase might prove more effective than chronic-phase treatment for limitation of infarct size. The first window of ischaemic preconditioning is mediated by opening of the KATP channel,[34] which is the mechanism of action of nicorandil; and the second window is mediated by nitric oxide and activation of G kinase, which is the mechanism of action of atrial natriuretic peptide.

Before this clinical trial, we had tested whether atrial natriuretic peptide could limit infarct size in a canine model in which the left anterior coronary artery was ligated for 90 min, followed by 6 h of reperfusion. Treatment with atrial natriuretic peptide reduced infarct size by about 40% after reperfusion (unpublished data). Our results are consistent with the finding of Hayashi and coworkers[20] that infusion of atrial natriuretic peptide immediately after reperfusion in patients with their first anterior acute myocardial infarction increased left ventricular ejection fraction.

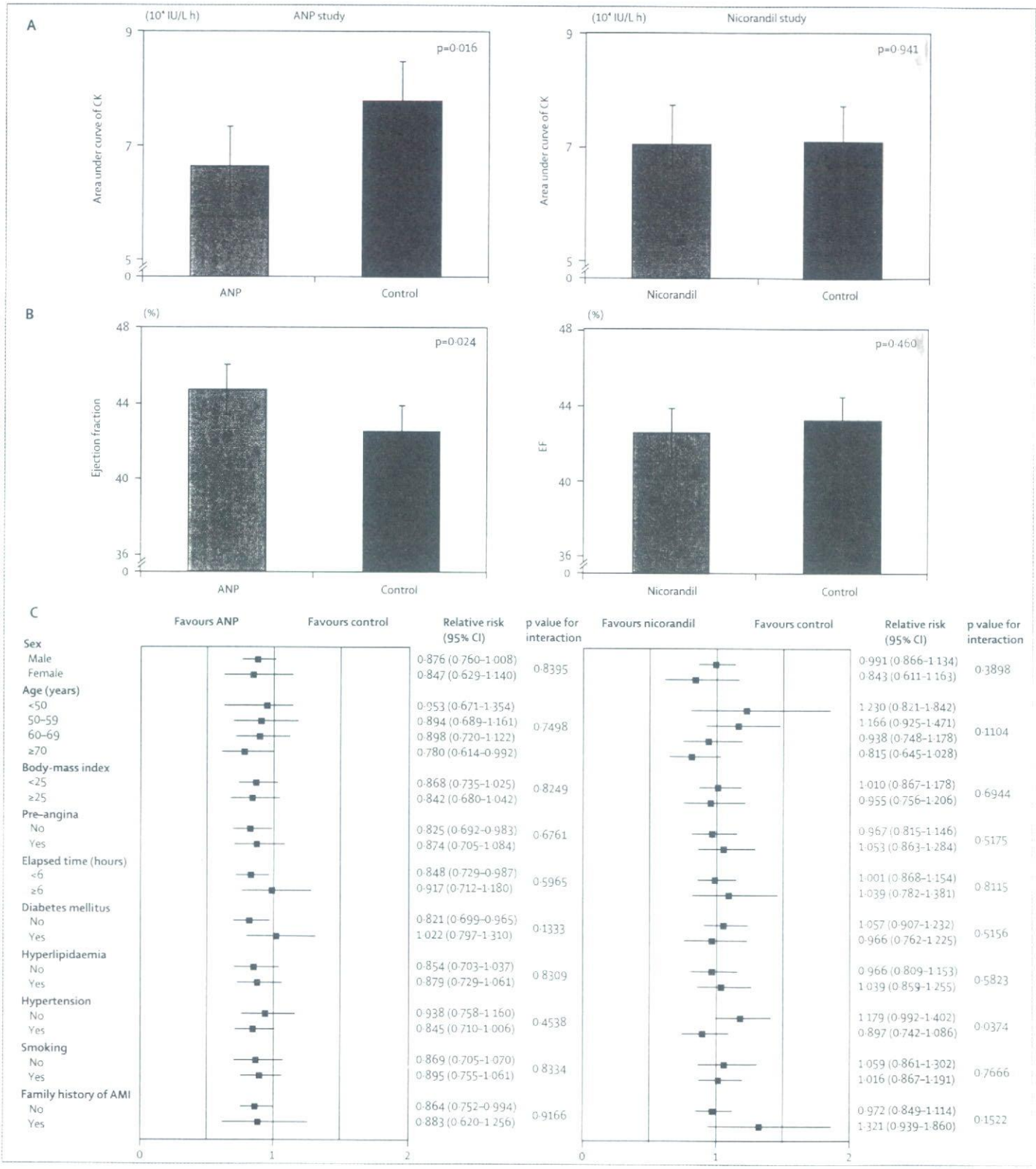

Figure 2: **Primary endpoints and subgroup analyses**
CK=creatine kinase. AMI=acute myocardial infarction. ANP=atrial natriuretic peptide. Panel A shows area under curve of creatine kinase concentration versus time. Panel B represents left ventricular ejection fraction measured at 6–12 months.

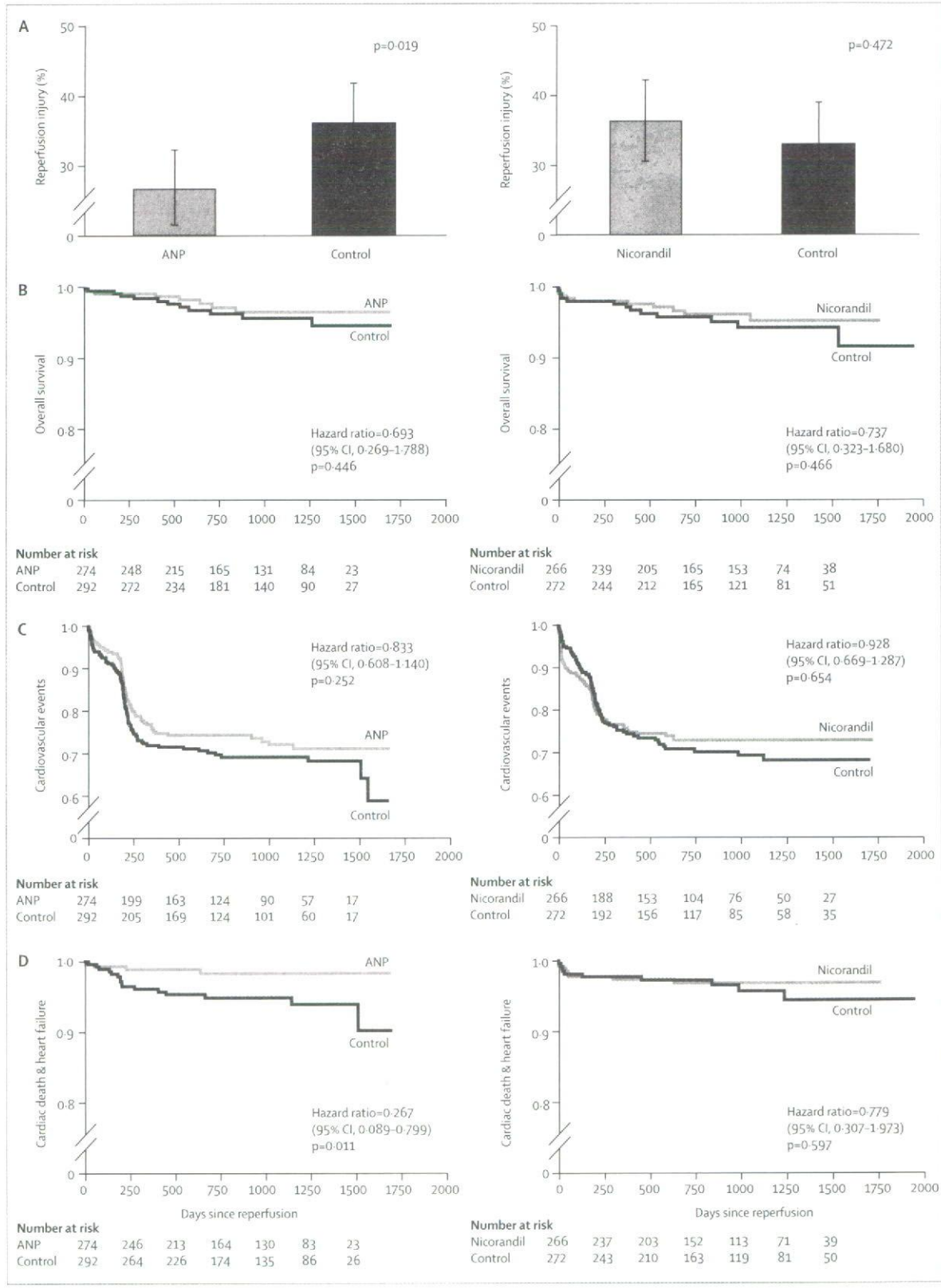

Figure 3: Secondary endpoints and other subanalyses
ANP=atrial natriuretic peptide.